RAGE-DEPENDENT SENSITIZATION OF THORACIC SENSORY NEURONS DURING INFLAMMATORY CONDITIONS

A Thesis Submitted to the College of Graduate Studies and Research
In Partial Fulfillment of the Requirements for the Degree of Master of Science
In the Department of Physiology
University of Saskatchewan, Saskatoon, SK

By

Manoj Nair G Baskaran

PERMISSION TO USE

By presenting this thesis in partial fulfilment of the requirements for a postgraduate degree from the University of Saskatchewan, I permit the libraries of this university may make it freely available for appraisal. I further agree that permission for copying of this thesis in any manner, either wholly or partially for scholarly purposes may be granted by the supervisors or committee members who supervised my work, or in their absence, by the Head of the Department or Dean of the College in which my thesis was completed. It is understood that the copying or publication of this thesis wholly or parts thereof for financial gain will not be allowed without my written permission. It is also understood that due recognition will be given to me and to the University of Saskatchewan in any scholarly use which may be produced from any material contained in my thesis.

Requests for permission to copy or make other use from material in this thesis either wholly or partially must be addressed to:

Head of the Department of Physiology

College of Medicine

University of Saskatchewan

Saskatoon, Saskatchewan S7N 0W5

ACKNOWLEDGEMENTS

I would like to express my utmost gratitude to my supervisors, Dr. Verónica Campanucci and Dr. Juan Ianowski. This work would have not been possible without your mentorship, knowledge and guidance. Thank you very much!

To Dr. George Katselis and his team (Paulos and Brooke), thank you for your support and guidance on the mass spectrometry work.

To my thesis committee members Dr. Francisco Cayabyab, Dr. Jennifer Chlan-Fourney and Dr. Sean Mulligan, thank you for the invaluable discussions and feedback that have greatly improved the value of this thesis.

To the members of the Campanucci (Zeinab, Andy and Rylan) and Ianowski Lab (Noman, Santosh, Jay, Nikolai and Paula) thank you for your friendship, support and thought-provoking discussions.

To the College of Medicine, thank you for the opportunity and support throughout my graduate program.

Last but not least, to my mom and dad, and friends, thank you for your solid support and encouragement!

TABLE OF CONTENTS

CHAPTER 3: RESULTS

CHAPTER 4: DISCUSSION AND CONCLUSION

LIST OF TABLES

LIST OF FIGURES

LIST OF ABBREVIATIONS

a.u.	arbitrary unit
ABC	ammonium bicarbonate
ACN	acetonitrile
ADAM10	a disintegrin and metalloproteinase domain-containing protein 10
AGE	advanced glycation end-products
ANOVA	analysis of variance
ASL	airway surface liquid
cAMP	cyclic adenosine monophosphate
CC	cytokine cocktail
CGRP	calcitonin gene-related peptide
COPD	chronic obstructive pulmonary disease
cRAGE	cleaved RAGE
Dia-1	diaphanous-1
DNA	deoxyribonucleic acid
DRG	dorsal root ganglion / ganglia
DTT	dithiothreitol
EC_{50}	half maximal effective concentration
EGTA	ethylene glycol-bis(β-aminoethyl ether)-N,N,N',N'-tetraacetic acid
ERK 1/2	extracellular signal–regulated kinases 1 and 2
ERK	extracellular signal–regulated kinase
esRAGE	endogenous secretory RAGE
ET-1	endothelin-1
FA	formic acid
HBSS	Hanks' balanced salt solution
HEPES	N-2-hydroxyethylpiperazine-N-2-ethane sulfonic acid
HMGB1	high mobility group-box protein 1

IAA	iodoacetamide
IB4	isolectin B4
Ig	immunoglobulin domain
IgC2-1	constant immunoglobulin domain 2, exon 4-6
IgC2-2	constant immunoglobulin domain 2, exon 7-8
IgV	variable immunoglobulin domain
IL-4	interleukin 4
IL-6	interleukin 6
IL-8	interleukin 8
LC-MS	liquid chromatography-mass spectrometry
LC-MS/MS	liquid chromatography-tandem mass spectrometry
LPS	lipopolysaccharide
MAPK	mitogen-activated protein kinases
mRNA	messenger ribonucleic acid
MgATP	adenosine 5'-triphosphate magnesium salt
MHC	major histocompatibility complex
***Mmus*RAGEv1**	*Mus musculus* receptor for advanced glycation-end products isoform 1
***Mmus*RAGEv2**	*Mus musculus* receptor for advanced glycation-end products isoform 2
MS	mass spectrometry
MS/MS	tandem mass spectrometry
MYD88	myeloid differentiation primary response 88
mβCD	methyl β-cyclodextrin
NADPH	nicotinamide adenine dinucleotide phosphate
NaV1.8	voltage-gated sodium channel subtype 1.8
NCBI	National Center for Biotechnology Information
NF-κB	nuclear factor κ B
NGF	nerve growth factor
PAMP	pathogen-associated molecular patterns

PCR	polymerase chain reaction
PKA	cyclic adenosine monophosphate-dependent protein kinase
PKC	protein kinase C
PKCβII	protein kinase C beta type II
PRR	pattern recognition receptor
qPCR	quantitative polymerase chain reaction
QTOF	quadrupole time-of-flight
RAGE KO	receptor for advanced glycation end-products-knock out
RAGE	receptor for advanced glycation end-products
ROS	reactive oxygen species
SCX	strong cation-exchange
SEM	standard error of the mean
Ser307	amino acid residue serine 307
Ser377	amino acid residue serine 377
SG	submucosal gland
siRNA	small interfering RNA
SP	substance P
sRAGE	soluble RAGE
Src	proto-oncogene tyrosine-protein kinase
tDRG	thoracic dorsal root ganglia
TFE	trifluororethanol
Th2	T helper type 2
Thr12	threonine 12 amino acid residue
Thr5	threonine 5 amino acid residue
TLR	toll-like receptor
TLR4	toll-like receptor 4
TNF-α	tumor necrosis factor α
TRPV1	transient receptor potential vanniloid 1

Tv1-RAGE	full-length receptor for advanced glycation end-products
V_{RM}	resting membrane potential
WT	wild-type

CHAPTER 1

INTRODUCTION

Airway diseases such as asthma, chronic obstructive pulmonary disease (COPD), cystic fibrosis, and bronchitis may arise from different etiologies but typically progress as a result of chronic inflammation (Hargreave and Parameswaran, 2006; Widdicombe and Wine, 2015). Inflammatory reaction to pathogens, irritants, and other stress-related substances is part of a normal protective physiological response of the airways which keeps the lung free of pathogens and noxious stimuli.

Foreign particles inhaled with each breath must be detected and removed to protect the airway. It is not surprising then, that a number of systems have evolved to detect and react to inhaled particles. Epithelial cells, immune cells and sensory neurons in the airway express receptors for noxious stimuli (such as bacterial products, irritants such as capsaicin (CAP), and many others). The detection of any of these signals trigger the release of paracrine factors or the release of neurotransmitters from nerve endings that in turn initiate an innate immune reaction. A central component of the innate airway defence against inhaled pathogens is the airway surface liquid (ASL; includes mucus) that facilitates mucociliary clearance.

During a bacterial infection, the airway epithelia, innate immune cells, and nerve endings detect bacterial products, such as lipopolysaccharide (LPS), and trigger the release of various inflammatory mediators including cytokines, chemokines, histamines, and eicosanoids that serve to recruit innate and adaptive immune responses (Talbot et al., 2016) and to produce copious volumes of ASL among other protective functions (Knowles and Boucher, 2002).

In this thesis, I investigated the effect of inflammatory signals on sensory neurons innervating the upper airways. Under inflammatory conditions these sensory neurons increase

ASL secretion from airway submucosal glands (SG), the source of ~95% of the ASL in upper airways (Wine, 2007). However, the underlying mechanisms that take place in sensory neurons under inflammatory conditions remain poorly understood. Therefore, I investigated the cellular mechanisms of sensory neuron sensitization in the dorsal root ganglia (DRG) of mice and the role of Receptor for Advanced Glycation End-products (RAGE). RAGE expression has been linked to chronic airway inflammatory pathologies (Sukkar et al., 2012), thus I have concentrated my research on the role of RAGE in mediating the response to bacterial products in modulating sensory neuron electrophysiological changes triggered in response to the bacterial product LPS. I also investigated changes in RAGE expression and the expression of RAGE variants, generated by alternative splicing, triggered by LPS in our preparation. Previous work has shown that in humans, murine and canine tissues RAGE undergoes alternative splicing which produces large transcriptomic and proteomic diversity of RAGE tissue-specific isoforms, however the significance of the spliced variants is unclear (Lopez-Diez et al., 2013).

Our results show that DRG neurons exposed to inflammatory conditions (i.e. LPS) develop a sensitivity to stimulation and produce stronger action potential firing. This response is absent in RAGE KO (receptor for advanced glycation end-products-knock out) cells, suggesting that the response to LPS is mediated by RAGE. Using mass spectrometry (MS)-based global proteomics, I identified the expression of the RAGE isoforms *Mmus*RAGEv1 and v2 (Lopez-Diez et al., 2013) specific to airway peripheral neurons under pathological inflammatory conditions (i.e. LPS). Thus, taken together, my results may contribute to the understanding of the role of neuronal stimulation of ASL hypersecretion in pathological conditions.

1.1 Neural innervation of airway SG

Neuronal stimulation is a major driver of ASL secretion during disease (Luan et al., 2014; Widdicombe and Wine, 2015). Most of the ASL produced in the upper airways emanates from airway SGs (Wine, 2007), which secretion is modulated/regulated by the airway intrinsic plexus. The airways intrinsic plexus is formed by sensory and autonomic fibers responsible for regulating airway function and maintaining homeostasis by compensatory reflexes (Fisher, 1964; Wine, 2007). Thus, the neural control of the airways is carried by parasympathetic (cholinergic) and sympathetic (adrenergic) reflex responses (Fig. 1.1) (Fischer et al., 2009; Hiemstra and Zaat, 2013).

ASL secretion by SG is under afferent control. The cell bodies of vagal afferent neurons are located in the nodose ganglion, and these neurons relay sensory information to the brain stem from which parasympathetic reflexes are initiated (Bautista et al., 2006; Springall et al., 1987; Widdicombe and Wine, 2015). In addition, sympathetic afferent and efferent fibers are also found in the vicinity of the SGs (Widdicombe and Wine, 2015). Sympathetic afferents travel with their efferent counterpart and their cell bodies reside in DRG from the thoracic (T1-T6) regions of the spinal cord (Dinh et al., 2004; Qin et al., 2007). Sympathetic and parasympathetic afferent neurons display many similarities. Other than their different anatomical locations, they both express typical sensory markers such as the transient receptor potential vanniloid 1 (TRPV1), substance P (SP), calcitonin gene related peptide (CGRP) and IB4 (Dinh et al., 2004; Plato et al., 2006; Zhang et al., 2008). It is generally accepted that the parasympathetic afferents have a stronger contribution since most of the known airway reflexes can be significantly suppressed by bilateral vagotomy. However, it has been recently postulated that these two afferent systems interact synergistically during inflammation, and thus, they can play a significant role in the regulation of the airways

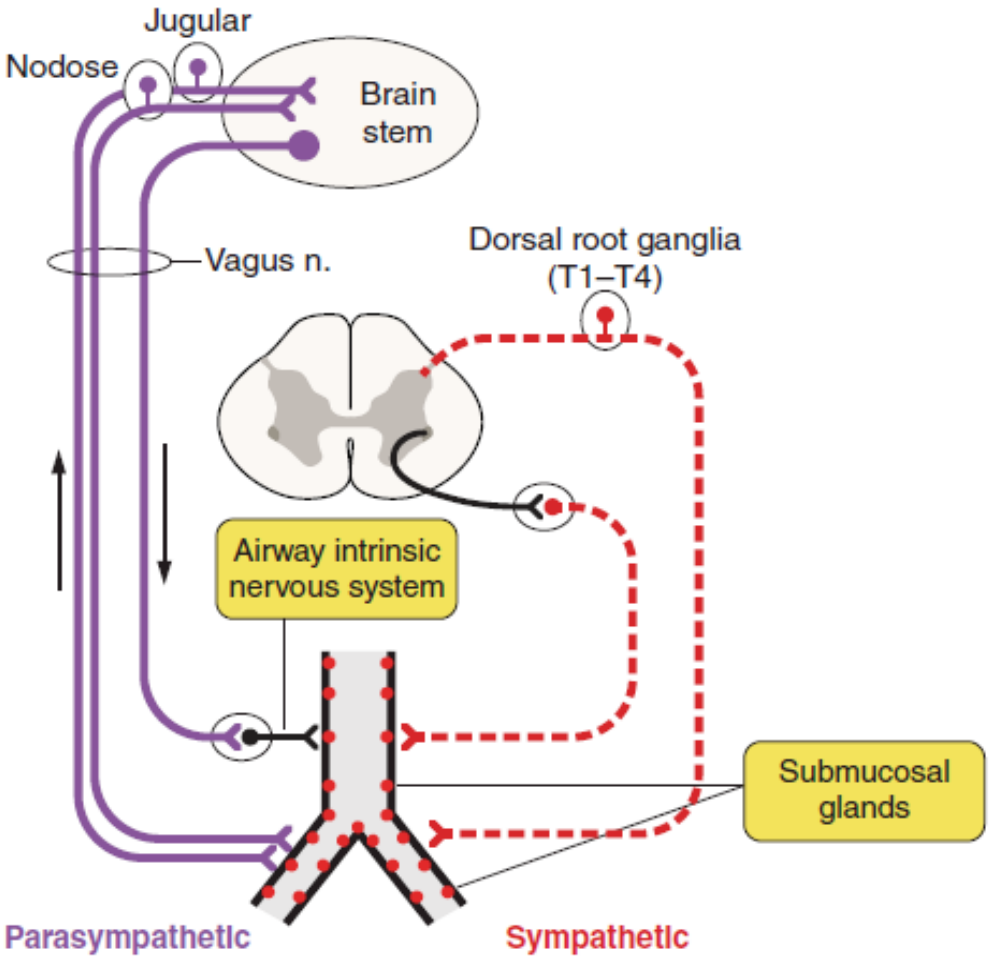

Figure 1.1 Neural innervation of airway SGs. Airway SGs receive parasympathetic (left) and sympathetic (right) inputs. Afferent fibers carry sensory information from the airways via the nodose and jugular ganglia to the brainstem nucleus tractus solitarius. Here, interneurons synapse with vagal preganglionic fibers that in turn excite intrinsic neuron-mediated SG ASL secretion. Sympathetic afferents transmit signals through DRGs from the thoracic segment T1-T4 whose axons terminate in Rexed Lamina II (substantia gelatinosa) of the dorsal horn. Interneurons of the substantia gelatinosa synapse with Rexed Lamina V efferent fibers that then stimulate SG ASL secretion. Reproduced from Widdicombe and Wine (2015).

under pathological conditions (Lee and Yu, 2014).

DRGs are nodule-like structures located in the intervertebral foramina that are dorsolateral to the spinal cord which relay information from the external environment to the central nervous system (CNS). Neurons within the DRGs are pseudo-unipolar cells with two bifurcations, which in the case of thoracic ganglia (tDRG), one projects peripherally to the lungs and heart; and the second projects centrally to the dorsal horn of spinal cord. Immunohistological studies on mouse lumbar DRGs showed heterogeneous populations of neuronal cell bodies with either unmyelinated C- (~70%) or myelinated Aβ-/Aδ- (~30%) fibers (Ruscheweyh et al., 2007) however, these proportions are uncertain in tDRGs. Aβ-fibers carry information related to touch and movement whereas Aδ-fibers are sensitive to chemical stimuli, noxious gases and inhaled particles, and inflammatory and immunologic mediators. C-fibers are sensitive to CAP, cigarette smoke, bradykinin, ozone, hypertonic saline and various other chemical stimuli. Both fiber types when stimulated produce reflex bronchoconstriction and increased cough to curb further noxious stimuli exposure, however, C-fibers can also increase vascular permeability and ASL production (Hamid et al., 2005). In the upper airways, afferent nerve endings arborize into the epithelial layer where depolarizations from various stimuli are transmitted through the neuronal cell body to vertical and radial interneurons (Todd, 2010) in the dorsal horn (Rexed Lamina II) of the spinal cord (Ordovas-Montanes et al., 2015). Subsequently, interneurons from these laminae dedicated to the modulation of noxious and non-noxious stimuli synapse onto Rexed Lamina VII efferent fibers (Todd, 2010). The activation of these efferent fibers contribute to the stimulation of ASL secretion from SG and also vasodilatation, plasma exudation, neuropeptide release and bronchoconstriction collectively termed as ‘neurogenic inflammation’ (Barnes, 2001; Undem and Carr, 2002).

1.1.1 Neurogenic inflammation and its contribution to ASL hypersecretion

In addition to orthodromic inputs to the spinal cord from sensory neurons, action potentials in sensory neurons can also be transmitted antidromically at branch points back down to the periphery. This constitutes the axon reflex, which together with sustained local depolarizations, lead to a rapid and local release of neural mediators from both peripheral axons and terminals (Sauer et al., 2001). Classic experiments by Goltz (1874) and Bayliss (1901) showed that electrically stimulating DRGs induced skin vasodilation, which led to the concept of a 'neurogenic inflammation', independent of that produced by the immune system. Neurogenic inflammation is mediated mainly by the release of the neuropeptides CGRP and SP from nerve endings, among other pro-inflammatory peptides, which act directly on vascular endothelial and smooth muscle cells (Brain and Williams, 1989; Edvinsson et al., 1987; McCormack et al., 1989; Saria, 1984). In addition to acting on the vasculature, these signals can act directly attracting and activating innate immune cells (mast cells, dendritic cells) and adaptive immune cells (T lymphocytes) (Ansel et al., 1993; Cyphert et al., 2009; Ding et al., 2008; Hosoi et al., 1993; Mikami et al., 2011; Rochlitzer et al., 2011) (see section 1.2). In the acute settings, neurogenic inflammation is protective, facilitating physiological wound healing and immune defense against pathogens by activating and recruiting immune cells. However, it is also likely to play major roles in the pathophysiology of allergic and autoimmune diseases by amplifying pathological or maladaptive immune responses. For example, in allergic airway inflammation sensory neurons have been shown to play a central role in initiating and augmenting the activation of innate and adaptive immunity (Caceres et al., 2009; Engel et al., 2011; Ostrowski et al., 2011).

Some studies suggest that during chronic inflammatory conditions, the DRG neurons of the sympathetic afferent pathway, including C-fibers, undergo sensitization (de Groat and

Yoshimura, 2009; Janig et al., 1996) which could potentially play a role in SG hypersecretion. DRG neurons become sensitized when exposed to pathogens known to affect the airways, such as the bacterial LPS. LPS binds to toll-like receptor 4 (TLR4), a member of the pattern-recognition receptor (PRR) family, that induces potentiation of TRPV1 currents, increased intracellular Ca^{2+} concentration (Diogenes et al., 2011) and the activation of signaling cascades that result in the activation of nuclear factor kappa B (NF-κB) and mitogen-activated protein kinases (MAPKs) (Tse et al., 2014). Thus, sensitized efferent sensory C-fibers, that innervate the SGs, can amplify inflammation and result in ASL hypersecretion in the airways by axon reflex through the release of neuropeptides on the airways during neurogenic inflammation (Barnes, 2001; Barnes et al., 1998; Maggi et al., 1995). During neurogenic inflammation, nociceptive C-fibers release various neuropeptides such as SP, neurokinin-A and CGRP as observed in guinea pig, rat and ferret studies through activation with the chilli pepper alkaloid, CAP (Hamid et al., 2005; Millqvist, 2000).

The role of sensory inflammation in the overproduction of ASL in airway diseases is supported by multiple pieces of evidence. For instance, SP is able to stimulate SG secretion in human airways *in vitro* and also goblet cell secretion in guinea pig airways through the activation of NK_1 (neurokinin 1)-receptors. Other factors that stimulate SG secretion are VIP (vasoactive intestinal peptide), cholinergic agonists, elevated cyclic adenosine monophosphate (cAMP), elevated Ca^{2+} and SP-induced acetylcholine release through enhancement of ganglionic transmission (Barnes, 2001). Despite evidences of neuropeptidergic factors as the key instigator of neurogenic inflammation and subsequent increased SG secretion in animal models, observations in *in vivo* human studies are poorly supportive of this hypothesis. This deviation may in part be due to species-specific pulmonary differences. For example, intra-epithelial SP- and CGRP-positive fibers make up more than 60% in guinea pigs as opposed to 1% in human airways

(Bowden and Gibbins, 1992). Some studies indicated increased SP in bronchial nerves from biopsies of fatal asthmatics while other studies were contradictory. Other considerations include plasticity-driven increased peripheral nerve innervation during inflammatory states mediated by neurotrophins secreted from inflammatory cells that may account for varied observations (Barnes, 2001). Given such inconsistencies, newer hypotheses have reappraised neurogenic inflammation to be the result of both immunological- and neurogenic-driven factors that could contribute to ASL hypersecretion. This neuro-immune hypothesis stems from the idea that although neurogenic inflammation is protective in the acute phase, chronic states tend to result in pathological or maladaptive immune responses (Chiu et al., 2012) which may enhance SG secretions in the airway.

1.2 Cooperative immunogenicity of the peripheral nervous and immune systems

The early understanding of immunogenicity involved responses of the immune system, excluding a role of the peripheral nervous system. However, emerging evidence strongly supports a role of the peripheral nervous system, since it shares identical and integrative protective mechanisms with the immune system. For instance, both systems express members of the PRR family that recognize a variety of highly conserved pathogen-associated molecular patterns (PAMP) (Santoni et al., 2015; Srikrishna and Freeze, 2009). These receptors, i.e. RAGE and toll-like receptors (TLR), are classified under the immunoglobulin (Ig) superfamily of cell surface molecules that initiate and amplify responses to inflammation, infection and injury in a tightly-regulated manner (Sukkar et al., 2012). However, in pathophysiological scenarios such as in chronic airway inflammation, over-active PRRs as a result of perturbed endogenous regulatory mechanisms can sensitize sensory fibers leading to unwanted consequences (Chiu et al., 2012). Sensory fibers are inherently capable of transmitting danger signals more readily than the mobilization of the innate immune system.

The high level of organization between neurons and airway structural cells suggests the likelihood of direct modification of inflammatory processes in the pulmonary system (McGovern and Mazzone, 2014).

In fact, research has shown that transient receptor potential cation channel, subfamily A, member 1 (TRPA1)-knockout mice that were exposed to the allergen ovalbumin, had no leukocyte infiltration in the airways, decreased cytokine and ASL production, and greatly attenuated airway hyper-reactivity (Caceres et al., 2009). Moreover, ablation of both TRPA1- and TRPV1-positive vagal mouse sensory neurons through genetic or pharmacological means caused a marked reduction in airway hyper-reactivity (Ordovas-Montanes et al., 2015). Such evidence suggests an intimate link between the peripheral nervous and immune systems. Thus, understanding the molecular mechanisms that underlie the coordinated interaction of peripheral neurons and immune cells may offer better therapies for airway inflammatory diseases.

1.2.1 RAGE and RAGE isoform expression

RAGE is a mammalian multiligand transmembrane receptor classified under the Ig superfamily. It contains one variable (V)- and two constant (C)-type extracellular domains, a transmembrane domain and a cytoplasmic tail (Lopez-Diez et al., 2013). The V-domain which contains two N-glycosylation sites is the primary binding site for most extracellular ligands. Intracellular signalling is mediated by the cytoplasmic tail through a common interaction with Dia-1 (diaphanous-1). *Ager*, the gene that codes for RAGE, is found on the locus for the MHC (major histocompatibility complex) Class III region on chromosome 6p21.31 in humans. Gene ancestry and protein mapping studies have indicated that *Ager* evolved from early Metazoans and its encoded protein contains

sequences that closely resemble cell adhesion proteins. The latter suggests that RAGE was first a cell adhesion protein before evolving into an inflammation-related receptor (Sessa et al., 2014).

RAGE was initially described as the receptor for advanced glycation end-products (AGEs), which form as the result of the non-enzymatic glycation of proteins in the presence of reducing sugars (Goldin et al., 2006). However, it is now evident that it also serves as a receptor for the calcium binding protein S100/calgranulin superfamily, high mobility group-box protein 1 (HMGB1), an amyloidogenic isoform of serum amyloid A and amyloid-β peptide (Lopez-Diez et al., 2013), and LPS (Rong et al., 2004). These interactions occur *in cis*, however *in trans* homophilic reactions with RAGE and other unbound RAGE forms, respectively, are also known to occur during cell-cell interaction (Sessa et al., 2014). RAGE has been linked to several inflammatory-related diseases such as diabetes and metabolic disorders, cardiovascular disorders, pulmonary disorders, neurologic disorders, including the aggressiveness of cancers. Cellular RAGE expression is readily detectable during embryonic development and decreases significantly upon cellular differentiation. Uniquely, this decrease is absent in lung tissue where its expression remains high under normal conditions and decreases in pathological states. Non-pulmonary differentiated tissues express low levels of RAGE and only increase under inflammatory conditions (Sparvero et al., 2009).

Several RAGE isoforms reported in human, murine and canine studies have revealed that variations of the Ig-V-domain can affect extracellular-ligand binding. Moreover, the lack of the transmembrane domain can result in a soluble form of RAGE that can be secreted. Isoforms that have a signal peptide can also be secreted or inserted into cell membranes. Secreted forms generated either through alternative messenger ribonucleic acid (mRNA) splicing or proteolytic cleavage of full-length RAGE (Tv1-RAGE) can play dual roles (Lopez-Diez et al., 2013). For

example, it can act as a "decoy receptor" in moderating inflammatory responses and can also promote inflammatory responses through interaction with Mac-1 (macrophage-1 antigen) (Sparvero et al., 2009). Bioinformatics has shown that there are 17 different RAGE isoforms (13 of which were recently identified – *Mmus*RAGE v1-13) in mice that are expressed in different levels in the brain, heart, kidney, liver, lung and pancreas. Tv1-RAGE mRNA contain exons 1 (SP), 2/3 (IgV domain), 4-6 (IgC2-1), 7-8 (IgC2-2), 9 (non-structural), 10 (transmembrane domain) and 11 (cytoplasmic tail). Other membrane-bound (have transmembrane domain) isoforms include *Mmus*RAGEv1 and mRAGE_v4. Conversely, likely soluble isoforms include *Mmus*RAGEv2 to v6.

1.2.2 Role of RAGE in neurogenic inflammation

RAGE has been recognized to play a central role in the airway inflammatory process based on molecular, biochemical and genomic studies (Mulrennan et al., 2015; Repapi et al., 2010; Sukkar et al., 2012). RAGE is ubiquitously expressed, and its up-regulation was firstly implicated in diabetes (Hofmann et al., 1999; Neeper et al., 1992; Schmidt et al., 1992; Yan et al., 2010), however, it has now been included as part of the pathological mechanisms active in multiple airway diseases, such as asthma, COPD, and cystic fibrosis (Buckley and Ehrhardt, 2010; Milutinovic et al., 2012). Among the multiple RAGE ligands, LPS, is known to induce ASL secretion through the innate immune and peripheral nervous systems (Alexander and Rietschel, 2001; Yamamoto et al., 2011; Yanagihara et al., 2001). Brochoalveolar lavage collected from ovalbumin-sensitized mice challenged with aerosolized LPS had higher IL-4 (interleukin 4) and tumor necrosis factor α (TNF-α) compared to controls (Qiao and Zhang, 2014). Airway epithelia of LPS-treated mice also displayed airway cell hyperplasia that is characteristic of airway inflammation (Toward and

Broadley, 2002; Vernooy et al., 2002). LPS cultured neonatal rat DRG neurons acutely exposed to LPS showed PKC (protein kinase C)- and PKA (cAMP-dependent protein kinase)-mediated CGRP release and increased intracellular Ca^{2+} (Hou and Wang, 2001). Interestingly, septic shock experiments involving RAGE KO mice that were intraperitoneally injected with LPS had attenuated serum levels of TNF-α, interleukin 6 (IL-6) and ET-1 (endothelin-1) compared to wild-type controls. In addition, the same group also showed through binding essays that LPS binds to the RAGE (Yamamoto et al., 2011). In humans, increased levels of RAGE have been observed in the alveolar walls of patients with COPD, and the up-regulation of RAGE also correlates with the expression of HMGB1, a transcription enhancer protein, in asthma patients (Sukkar et al., 2012; Zhou et al., 2012). The latter is consistent with the decreased antigen-induced airway inflammation and hyporesponsiveness in RAGE KO mice model of asthma (Lee et al., 2013). HMGB1 can bind to RAGE and other TLRs to initiate a cascade of events that activate NF-κB which in turn induces cytokine production and promotes inflammation. It has been hypothesized that RAGE and TLRs may have collaborative signalling through myD88-dependent pathways that tend to elicit stronger inflammatory responses than TLR-exclusive pathways (Hall and Agrawal, 2015). The interaction between RAGE and its ligands induces reactive oxygen species (ROS) accumulation, probably through NADPH (nicotinamide adenine dinucleotide phosphate) oxidase (Ruderman et al., 1992; Schmidt et al., 1994; Vincent et al., 2007; Wautier and Schmidt, 2004). Thus, the activation of NF-κB perpetuates oxidative stress and together with other pro-inflammatory factors generate the inflammatory state in neurons (Tobon-Velasco et al., 2014). Alternatively, sensitized RAGE KO mice challenged with ovalbumin displayed reduced eosinophilic inflammation and goblet cell metaplasia, decreased Th2 (T helper type 2) cytokine production, and lower numbers of pulmonary innate lymphoid cells compared to controls (Taniguchi et al., 2015).

1.3 Rationale and Hypothesis

During inflammatory conditions, sensory neurons innervating the SGs in the upper airways contribute to ASL secretion. It is not clear however, whether sympathetic afferent neurons play a role, and if so, to what extent in the regulation of ASL secretion under inflammatory conditions.

My working ***hypothesis*** is that under inflammatory conditions, RAGE expression and signalling mediates tDRG neuron sensitization. In particular, I propose that exposure to LPS will cause an increase in CAP-evoked current parameters in neurons from WT mice, but these changes will not be expected in neurons from RAGE KO mice. Similarly, we propose that evoked action potential generation will be increased in neurons from WT, but not from RAGE KO, mice when exposed to LPS. Furthermore, I propose that changes in the expression pattern of RAGE isoforms underlie the sensitization of tDRG neurons during LPS exposure. Here, I expect to see an increase in full length RAGE (Tv1-RAGE) expression, however the expression pattern of RAGE isoforms in membrane and cytosolic fractions is unknown and cannot be speculated.

CHAPTER 2

MATERIALS & METHODS

2.1 Animals. A colony of RAGE KO mice on a C57BL/6 background was maintained by breeding heterozygous mice as previously described (Chandna et al., 2015). Heterozygous mice were generated by back-crossing RAGE KO (homozygous) mice (Myint et al., 2006) with C57BL/6 wild type (WT) mice. All experiments were based on tDRGs (T1-T4) from homozygous (RAGE KO) mice and their C57BL/6 (wild type) littermates. Mice were genotyped using genomic DNA (deoxyribonucleic acid) and PCR (polymerase chain reaction) as previously described (Myint et al., 2006) but with slight modifications. Briefly, ~2 mm of mouse tail was digested for 30 mins at 95^{o}C in 300 µL digestion buffer (0.5 M EDTA (ethylenediaminetetraacetic acid) and 50% NaOH dissolved in distilled water). Samples were chilled on ice for 5 mins before the addition of 75 µL neutralization buffer (40 mM Tris-HCl (tris hydrochloride)). Samples were vortexed briefly and 2 µL was used for PCR (20 µL reaction) (Truett et al., 2000). PCR reactions were run on 2% agarose gels containing 0.5 µg/mL ethidium bromide and visualized on a UV (ultraviolet)-illuminated gel box. All *in vitro* experiments were done with neonatal pups (P0–P4). This work was approved by the University of Saskatchewan's Animal Research Ethics Board (Campanucci: protocol 20090082) and adhered to the Canadian Council on Animal Care guidelines for humane animal use.

2.2 Primary tDRG cultures. Bilateral tDRG (T1-T4) neurons were harvested and cultured from neonatal (P0-P4) mice as previously described for peripheral neurons (Campanucci et al., 2008). tDRG neurons were selected as they are known to innervate the upper airways

(Widdicombe and Wine, 2015). Briefly, ganglia were removed under sterile conditions and enzymatically dissociated at 37°C in HBSS (Hanks' balanced salt solution) containing trypsin (180–200 U/mL; Worthington, Freehold, NJ, USA) and buffered with HEPES (N-2-hydroxyethylpiperazine-N-2-ethane sulfonic acid; pH 7.4). The resulting cell suspension was washed twice in serum-containing Leibovitz's L-15 medium to inactivate the trypsin and plated on laminin-coated glass bottom petri dishes (35 mm) made in-house. The neurons were grown in L-15 medium supplemented with vitamins, cofactors, penicillin–streptomycin, 5 mM glucose, 5% rat serum and NGF (nerve growth factor; 10 ng/mL). Cultures were maintained at 37°C in a humidified atmosphere of 95 % air-5 % CO_2 and fed every 4 days with growth media. To eliminate non-neuronal cells, cultures were treated with cytosine arabinoside (10 µM; Sigma-Aldrich, St. Louis, MO, USA) from days 2 to 4. Established DRG cultures were incubated for 24h at 37^{o}C; (5% CO_2; humidified) in growth media alone (control), with a cytokine cocktail (CC) consisting of 1.5 nM IL-6 (Murata et al., 2011; Suto et al., 1993), 1.5 nM IL-8 (interleukin 8) (Dong et al., 2012), 3 nM TNF-α (Hensellek et al., 2007) and 0.6 µM IL1-β (interleukin 1 beta) (Saleh et al., 2013) or with 1µg/mL LPS (Sigma-Aldrich)-supplemented growth media. Both CC and LPS pro-inflammatory inducers were tested in WT tDRGs for their ability to produce robust and reproducible CAP-evoked currents that were indicative of inflammation (increased peak amplitude, current density and charge). Of these two inducers, I chose LPS for this study as it not only met the requirements mentioned but was also easier to prepare.

2.3 Whole-cell Patch Clamp Electrophysiology. Medium-sized tDRG neurons (~25-35 µm) were selected for whole-cell recording. Membrane currents were recorded with an Axopatch 200B amplifier (Molecular Devices, Palo Alto, CA, USA) equipped with a 1 GΩ cooled head-stage

feedback resistor and a Digidata 1400A analog-to-digital converter (Molecular Devices), and stored on a personal computer. Current- and voltage-clamp protocols, data acquisition, and analysis were performed using pClamp 10 (Molecular Devices) and Origin 9.0 software (OriginLab Corporation, Northampton, MA, USA). Patch pipettes were made using thin-wall borosilicate glass capillaries (World Precision Instruments, FL, USA) using a vertical puller (PC 10; Narishige Scientific Instrument Lab., Tokyo, Japan) and polished with a microforge (Narishige) to a final resistance of 3–8 MΩ when filled with intracellular recording solution. In most experiments, 75% of the series resistance was compensated, and junction potentials were cancelled at the beginning of the experiment. Recording electrodes were filled with the following intracellular solution (in mM): 65 KF, 55 $KC_2H_3O_2$, 5 NaCl, 0.2 $CaCl_2$, 1 $MgCl_2$, 10 EGTA (ethylene glycol-bis(β-aminoethyl ether)-N,N,N',N'-tetraacetic acid), 2 MgATP (adenosine 5'-triphosphate magnesium salt) and 10 HEPES, and pH was adjusted to 7.2 with KOH (all from Sigma-Aldrich). Cultured neurons were perfused continuously at 1 mL/min with control perfusion solution consisting of (in mM): 140 NaCl, 5.4 KCl, 0.33 NaH_2PO_4, 0.44 KH_2PO_4, 2.8 $CaCl_2$, 0.18 $MgCl_2$, 10 HEPES, 5.6 glucose, 2 glutamine, 0.001% atropine and 5 μg/mL phenol red; pH was adjusted to 7.4 with NaOH (all from Sigma-Aldrich). Whole-cell patched neurons were allowed to stabilize for 5 min before recording. Action potentials were generated in current-clamp mode by injection of a series of depolarizing current steps at 100 pA increments for 500 ms. All other experiments were carried out under voltage-clamp mode. A fast-step perfusion system was used to deliver either control or CAP (1μM)-containing extracellular solution at 1 mL/min perfusion rate.

2.4 MS-based proteomic analyses. MS-based proteomic analysis was used to study global protein changes in tDRG neurons from WT mice in control or LPS conditions. This method was preferred over Western Blotting or qPCR (quantitative polymerase chain reaction) because no RAGE isoform-specific antibodies are available and qPCR is unable to detect posttranslational modifications, respectively.

Suspensions of cultured tDRG neurons from WT and RAGE KO mice were prepared as described above, and plated onto specialized cell culture dishes (Sarstedt, Nümbrecht, Germany). We used approximately 80,000 cells per experimental group (control or LPS), each plating is generated from 20 pups. Membrane and soluble fractions from cultured tDRG neurons were obtained using the ProteoExtract Native Membrane Protein Extraction Kit (EMD Millipore, MA, USA) and processed as per the manufacturer's instructions and stored at -80^{o}C. Protein concentrations were determined by Nanodrop analysis with a BioTek Synergy HY multi-detection plate reader (Winooski, VT, USA).

2.4.1 In-solution Digestion. Protein samples were concentrated by acetone precipitation. To precipitate proteins, 4x sample volume of cold (-80^{0}C) acetone was added to an aliquot from lysate, vortexed, and incubated overnight at -80^{0}C. Then samples were centrifuged 13000 x *g* at 4^{0}C for 15 min. After washing protein pellets twice with cold (-80^{0}C) 80% acetone/20% water, protein pellets were air dried and re-suspended in 55 µL trifluoroethanol (TFE) buffer (10% TFE, 100 mM ammonium bicarbonate (ABC)). Proteins were digested in-solution using an in-house developed protocol. Briefly, 45 µL of each protein sample was placed in 1.5 mL tube and diluted with 5 µl of 100 mM ABC buffer (Fisher Scientific, Fair Lawn, NJ, USA) and 50 µL TFE (Fisher Scientific) to denature proteins. The samples were treated with 1 µL of 1M DTT (dithiothreitol) (MP

Biomedicals, Solon, OH, USA) while shaking at 300 RPM (Eppendorf Thermomixer, Eppendorf, Mississauga, ON, Canada) at 60^{o}C for 60 min to reduce disulfide bonds formation. Next, samples were alkylated with 100 µL of 110 mM iodoacetamide (IAA; Fisher Scientific) at 37^{o}C for 30 min on a shaker, covered with aluminum foil, to prevent further disulfide bond formation. The samples were dried in a speedvac (Labconco, Kansas City, MO, USA). Proteins in the samples were treated with 1 mL cold acetone followed by refrigeration at -80^{o}C for 60 min to eliminate salts and other interfering compounds (e.g. detergents), which can prevent digestion. The samples were centrifuged twice at 18000 x *g* for 30 min and acetone was carefully removed. Next, samples were dried in a speedvac and a buffer-containing trypsin (Promega Corporation, Madison, WI, USA) solution (50 ng/µL trypsin in 1 mM HCl (hydrochloric acid) /100 mM ABC) was added to the samples in a 40:1 protein:trypsin. The samples were incubated in a shaker at 300 RPM overnight at 37^{o}C. Trypsin buffer at the same ratio was added again in the morning to ensure complete digestion of proteins into peptides. After 2 hrs of further incubation at 37^{o}C, digested peptides were dried in speedvac and stored at -80^{o}C until further analysis.

2.4.2 Strong Cation Exchange (SCX)-based Fractionation. SCX-based fractionation was performed using SCX SpinTips sample prep kit (Protea Biosciences, Morgantown, WV, USA). The digested protein samples were dissolved in 200 µL of SCX reconstitution solution, a pH of 3 was adjusted with formic acid (FA). The samples were then loaded on to SCX SpinTip and centrifuged at 2000 x *g* for 6 min. To enhance peptide binding to SCX SpinTip samples were centrifuged 3 times. The flow through at the end of the step was transferred to a 1.5 mL tube for MS analysis. Peptides bound to SCX column were eluted using stepwise concentrations (in M): 20, 40, 60, 80, 100, 150, 250, 500 of ammonium formate (Sigma-Aldrich) in 10% acetonitrile

(ACN; Fisher Scientific) at pH 3. 150 µL of ammonium formate (in increasing concentrations) was added to the SpinTip and centrifuged at 2000 x *g* for 6 min. The flow through was collected after every centrifugation and transferred to 1.5 mL tube. All flow through were dried in speedvac and stored at -80^{o}C.

2.4.3 MS Workflow. All SCX fractions containing tryptic peptide were reconstituted in 20 µl of MS grade water:ACN:FA (97:3:0.1 v/v) followed by vortexing for 1-2 min. The resulting solutions were centrifuged at 18000 x *g* for 10 min at 4ºC. 15 µL aliquot of each sample was transferred to a mass spectrometry vial (Agilent Technologies Canada Ltd., Mississauga, ON, CA) for liquid chromatography-tandem mass spectrometry (LC-MS/MS) analysis. All MS analyses were performed on an Agilent 6550 iFunnel quadrupole time-of-flight (QTOF) mass spectrometer equipped with an Agilent 1260 series liquid chromatography instrument and a Chip Cube LC-MS (liquid chromatography-mass spectrometry) interface (Agilent Technologies). Chromatographic peptide separation was accomplished using a high-capacity high performance liquid chromatography (HPLC)-Chip II: G4240-62030 Polaris-HR-Chip_3C18 consisting of a 360 nL enrichment column and a 75 µm × 150 mm analytical column, which were both packed with Polaris C18-A, 180Å, 3 µm stationary phase. Samples were loaded onto the enrichment column with 50% solvent A (0.1% FA in water) and 50% solvent B (0.1% ACN:FA) at a flow rate of 2.0 µL/min. Samples loaded to enrichment column were transferred onto analytical column, and peptides were separated with linear gradient solvent system. The linear gradient program was employed for peptide separation with solvent A and solvent B on an analytical column. The linear gradient is 3–25% solvent B for 50 min and then 25–90% solvent B for 10 min at a flow rate of 0.3 µL/min. Positive-ion electrospray MS data was acquired using a capillary voltage set at 1900

V, the ion fragmentor set at 360 V, and the drying/collision gas (nitrogen) set at 225ºC with a flow rate of 12.0 L/min. Spectral results were collected over a mass range of 250–1700 mass/charge (m/z) at a scan rate of 8 spectra/sec. Tandem mass spectrometry (MS/MS) data were collected over a range of 100–1700 m/z and a set isolation width of 4 atomic mass units. The top 20 most intense precursor ions for each MS scan were selected for MS/MS with active exclusion for 0.25 min. To clarify, precursor ions are of a specific m/z ratio in the first stage (MS) of MS/MS. These ions will then undergo collision-induced dissociation using nitrogen gas in the second stage (MS/MS) of MS/MS.

2.4.4 Protein Identification. Spectral data were converted to a m/z data format using Agilent MassHunter Qualitative Analysis Software (Agilent Technologies) and were processed against the NCBI (National Center for Biotechnology Information) non-redundant *Mus musculus* database, using SpectrumMill (Agilent Technologies) as the database search engine. Search parameters included a fragment mass error of 50 parts per million (ppm), a parent mass error of 20 ppm, trypsin cleavage specificity, and carbamidomethyl as a fixed modification of cysteine. In addition, four stages of database search in variable modification mode were carried out with different sets of variable modifications. In first stage, carbamylated lysine, oxidized methionine, pyroglutamic acid, deamidated asparagine and phosphorylated serine, threonine, and tyrosine were set as variable modifications. In the second stage, validated hits from the first stage were searched using the following variable modifications: acetyl lysine, oxidized methionine, pyroglutamic acid, deamidated asparagine, and phosphorylated serine, threonine, and tyrosine. The validated hits from the second stage were searched using semi-trypsin non-specific C-terminus, yielding the third stage validated hits, which were subsequently searched using semi-trypsin non-specific N-

terminus (fourth stage), with no other variable modifications specified. After each stage, Spectrum Mill validation was performed at peptide and protein levels (1% false discovery rate).

Protein samples were reduced, alkylated and digested with trypsin in-solution in accordance with a modified version of a previously published protocol (Zhang et al., 2011). Tryptic peptides were analyzed by LC-MS/MS using an Agilent HPLC Chip/6550 iFunnel QTOF mass spectrometer (Agilent Technologies). MS/MS were referenced against the mouse NCBI non-redundant database and a custom database (containing mouse RAGE protein isoforms) using Spectrum Mill (Fig. 2.1). Spectral counts were used to report relative quantitation of proteins.

2.4.5 Manual Identification of Unique Modified RAGE isoforms (see Fig. 2.1). For either genotype, tryptic peptides identified in each RAGE isoform from the custom database in each treatment group were sorted according to their sequences. Then, common and duplicate peptides found in 2 or more RAGE isoforms were discarded leaving behind unique peptides that were specific to a particular RAGE isoform. Finally, these peptides were further specified according to their post-translational modifications.

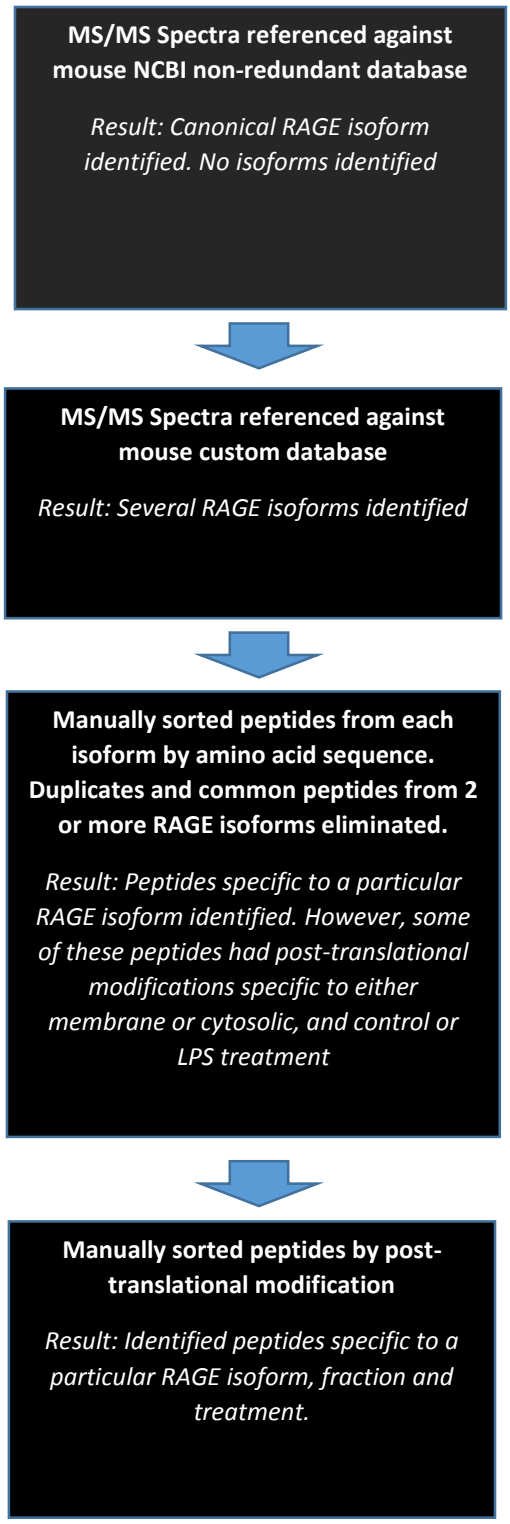

Figure 2.1 Processing of MS/MS spectra in the identification of unique post-translationally modified RAGE isoform peptides in WT tDRG neurons under control and LPS treatment conditions.

2.5 Statistical Analyses. We compared the EC_{50} (half maximal effective concentration) obtained from the dose response curves using tDRG neurons from either WT and RAGE KO, by unpaired *t*-test with Welch correction. In voltage-clamp experiments, raw values of peak amplitude, current density and charge of CAP-evoked current were compared using the unpaired *t*-test with Welch correction. In current-clamp experiments, action potential counts were compared using Mann-Whitney test. Resting membrane potentials (V_{RM}) were compared using the Kruskal-Wallis test (non-parametric analysis of variance, ANOVA). The significance threshold was set at 0.05 for all statistical tests performed.

CHAPTER 3

RESULTS

3.1 Determination of working concentration for CAP-evoked currents

In order to test the possible sensitization of sensory neurons exposed to inflammatory conditions (i.e. LPS-treatment or cytokines), we studied neuronal excitability in response to the injection of depolarizing current and to applications of the agonist CAP. Thus, to determine a submaximal working concentration of CAP, that would allow us to observe potential increases or decreases in whole-cell currents, we generated a dose-response curve to increasing concentrations of CAP in tDRG cultured neurons from WT and RAGE KO mice (Fig. 3.1). Cultured neurons were briefly exposed to CAP (0.1, 0.5, 1, 2.5, 5 and 10 µM; 1s) and the data were fitted with a logistic Hill function (R^2=0.93746 for WT, and R^2=0.94002 for RAGE KO). The EC_{50} of CAP obtained in cultures from WT and RAGE KO mice was 1.50 ± 0.44 µM and 2.25 ± 0.81 µM, respectively. No significant difference (p>0.05) was found in the EC_{50} values between the two genotypes. Subsequently, 1 µM CAP was selected as the submaximal working concentration throughout the study.

3.2 Exposure of sensory neurons to cytokines cocktail induces sensitization of CAP-evoked currents

Cultured tDRG neurons from WT mice were incubated in either control or cytokine cocktail (CC)-containing growth media (for 24 hr) before whole-cell recording of CAP-evoked currents. The mean peak amplitude of CAP-evoked currents in CC-treated neurons (-1063.51 ± 170.34 pA) was significantly higher (p<0.05) than in control neurons (-554.04 ± 64.01 pA) (Fig. 3.2A, B). Mean

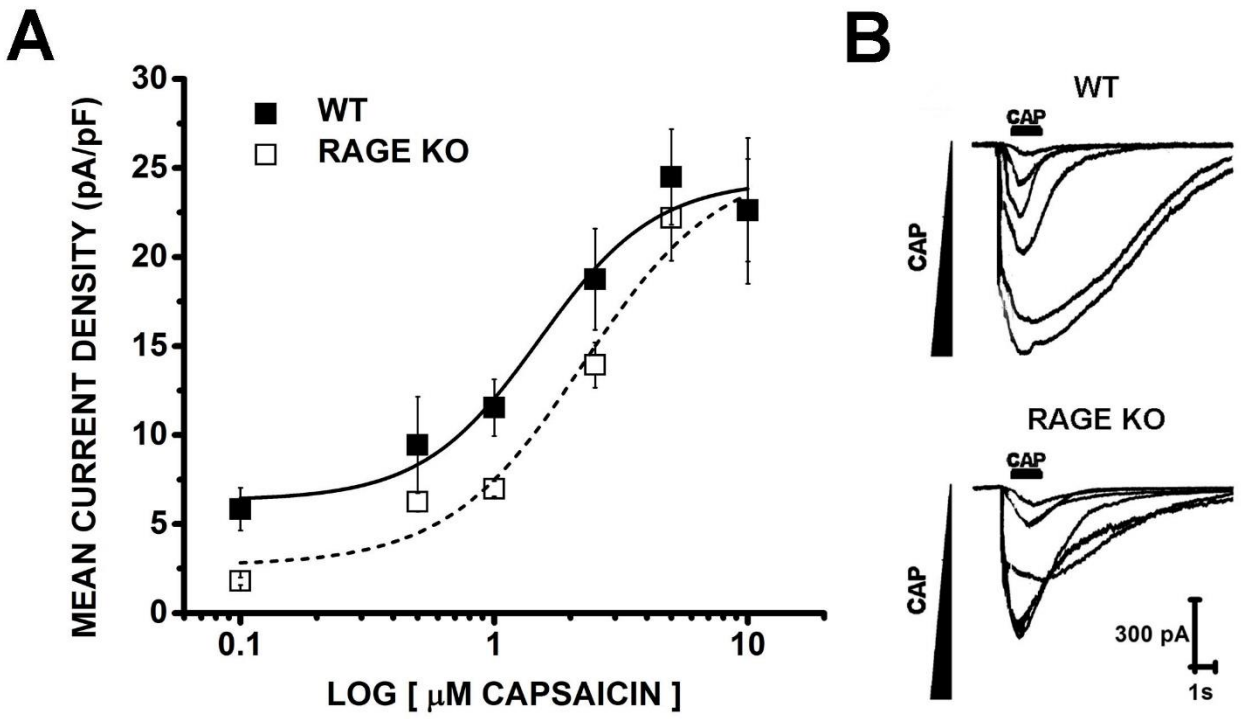

Figure 3.1 Dose-response of CAP-evoked currents in WT and RAGE KO DRG neurons. Dose dependency of CAP-evoked currents from cultured tDRG neurons from wild-type (WT) and RAGE-knockout (RAGE KO) mice (P0-P4) obtained by whole-cell patch clamp electrophysiology. DRGs neurons were clamped at -60mV and exposed to CAP for 1s. Data points indicate mean current density (pA/pF) at 0.1 (n = 6 for each genotype), 0.5 (WT=7; RAGE KO=6), 1 (WT=11; RAGE KO=10), 2.5 (WT=6; RAGE KO=7), 5 (WT=5; RAGE KO=8) and 10 μM CAP (WT=5; RAGE KO=7). The data were fitted with a logistic Hill function – WT R^2=0.93746; RAGE KO R^2=0.94002. Error bars indicate mean ± SEM. The EC_{50} of CAP in wild-type and RAGE KO was 1.50 ± 0.44 μM and 2.25 ± 0.81 μM, respectively.

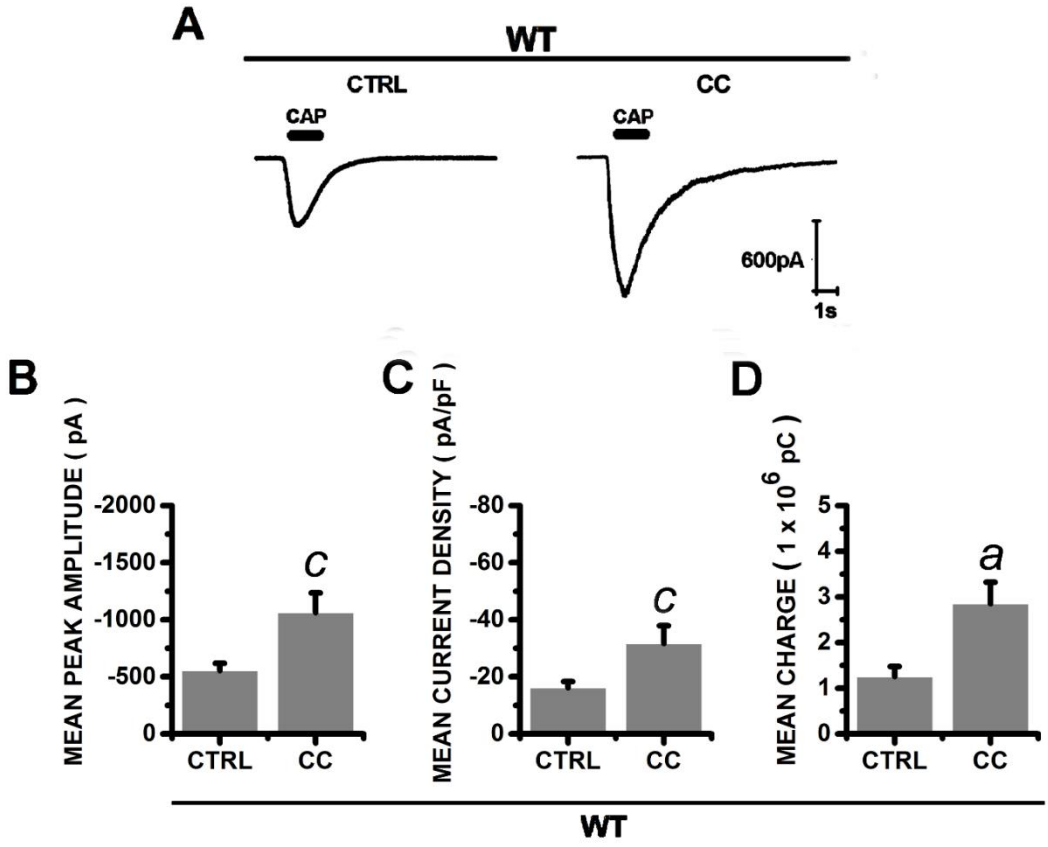

Figure 3.2 CC exposure increases CAP-evoked currents in tDRG neurons from WT neonatal mice. The CC consisted of 1.5 nM IL-6 (Murata et al., 2011; Suto et al., 1993), 1.5 nM IL-8 (Dong et al., 2012), 3 nM TNF-α (Hensellek et al., 2007) and 0.6 μM IL1-β (Saleh et al., 2013). **(A)** Representative CAP (1 μM; 1 s)-evoked current traces (V_H = -60 mV) from cultured wild type (WT) tDRGs. **(B)** Mean peak amplitude (pA), **(C)** current density (pA/pF) and **(D)** charge (1 x 10^6 pC) graphs of WT DRG neurons exposed to either control or CC-containing media (24h). Treatment groups (mean peak amplitude, mean current density, mean charge): WT control (13); WT CC (10). Error bars indicate mean ± SEM. Letter '*a*' denotes $p<0.01$ and '*c*' denotes $p<0.05$ based on unpaired *t*-test with Welch correction. Control group is abbreviated as 'CTRL'.

current density was significantly higher ($p < 0.05$) in the CC group (-31.73 ± 6.13 pA/pF) compared to controls (-16.19 ± 2.16 pA/pF) (Fig. 3.2A, C). The mean charge was significantly higher ($p < 0.01$) in the CC group (2.70 ± 0.35 x 10^6 pC) compared to controls (1.26 ± 0.22 x 10^6 pC) (Fig. 3.2A, D). The results indicate that DRG neurons exposed to proinflammatory cytokines, modeling the conditions of a diseased airway, develop sensitization and become hyperresponsive to stimulation.

3.3 RAGE expression is required for the potentiation of CAP-evoked currents in tDRG neurons

To generate inflammatory conditions that are physiologically more relevant to airways pathology, we expossed cultured tDRG neurons to the bacterial endotoxin LPS. Thus, cultured neurons from WT and RAGE KO mice were incubated in either control or LPS-containing growth media (for 24 hr) before the recording of whole-cell CAP-evoked currents. Consistent with our results with the CC-containing media, the mean peak amplitude of CAP-evoked currents in LPS-treated neurons from WT mice (-1188.54 ± 177.76 pA) was significantly higher ($p<0.01$) than in control neurons (-554.04 ± 64.01 pA) (Fig. 3.3A, B). To account for neuronal size we calculated the mean current density, which was significantly higher ($p < 0.005$) in the LPS group (-49.49 ± 7.38 pA/pF) compared to controls (-16.19 ± 2.16 pA/pF) (Fig. 3.3A, C). Consistently, the mean charge was significantly higher ($p < 0.005$) in the LPS group (2.70 ± 0.35 x 10^6 pC) compared to controls (1.26 ± 0.22 x 10^6 pC) (Fig. 3.3 A, D). Contrasting with our results in neurons from WT mice, tDRG neurons from RAGE KO mice did not exhibit significant differences in CAP-evoked currents in the LPS group compared to controls ($p>0.05$) (Fig. 3.3A-D). Mean peak amplitude for control

group was 282.13 ± 43.79 pA and LPS-treated group was 349.77 ± 41.71 pA (Fig 3.3A, B). Mean current density for control (-9.00 ± 0.88 pA/pF) and LPS-treated (–10.94

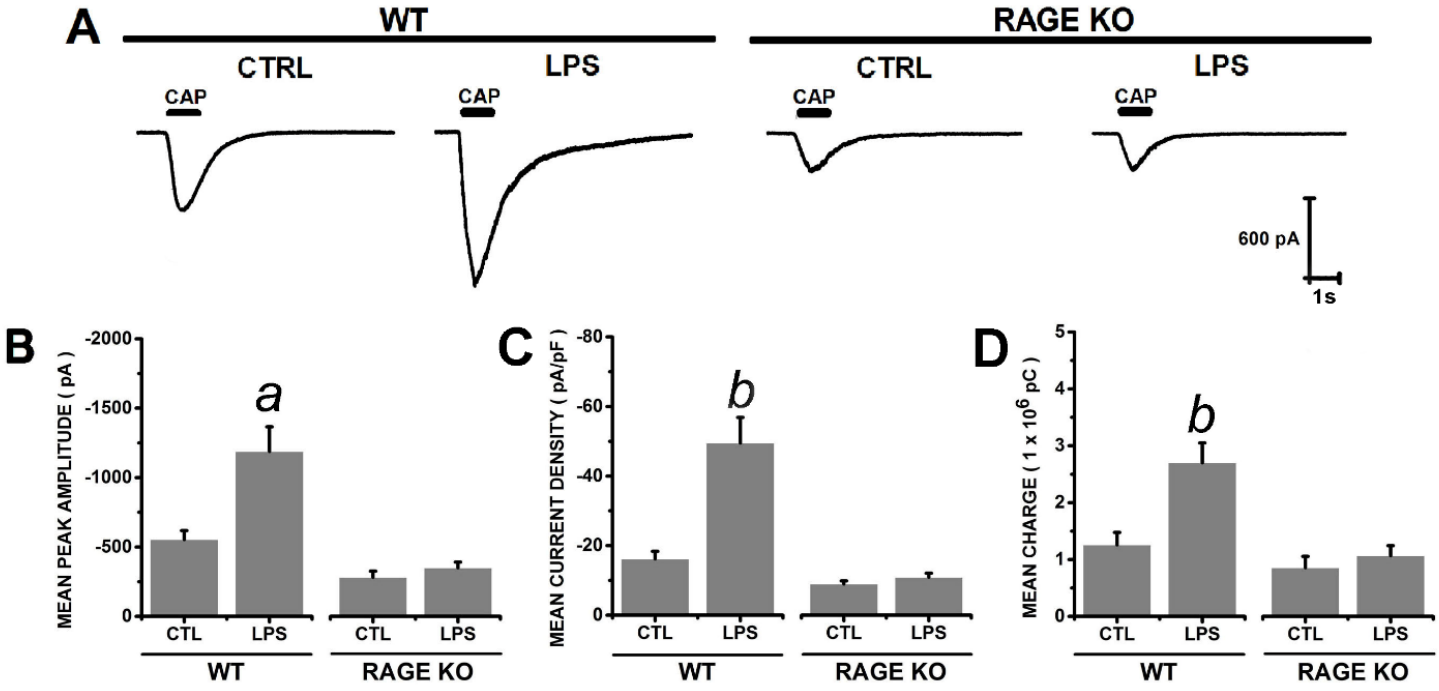

Figure 3.3 LPS exposure increases CAP-evoked currents in tDRG neurons from WT neonatal mice. (A) Representative CAP (1 µM; 1 s)-evoked current traces (V_H = -60 mV) from cultured wild type (WT) and RAGE-knockout (RAGE KO) tDRGs. **(B)** Mean peak amplitude (pA), **(C)** current density (pA/pF) and **(D)** charge (1 x 10^6 pC) graphs of WT and RAGE KO DRG neurons exposed to either control or LPS-containing media (1 µg/mL; 24h). Treatment groups (mean peak amplitude, mean current density & mean charge): WT control (13); WT LPS (9); RAGE KO control (8); RAGE KO LPS (9; *Exception: n=8 for Mean Charge in RAGE KO LPS group*). Error bars indicate mean ± SEM. Letter '*a*' denotes $p<0.01$ and '*b*' denotes $p<0.005$ based on unpaired *t*-test with Welch correction. Control group is abbreviated as 'CTRL'.

± 1.14 pA/pF) groups (Fig. 3.3 A, C) were not significantly different (p>0.05). Similarly, the mean charges for the control group (0.86 ± 0.20 x 10^6 pC) was not significantly different (p>0.05) from the LPS-treated group (1.07 ± 0.18 x 10^6 pC) (Fig. 3.3A, D).

3.4 RAGE expression is required to increase neuronal excitability in tDRG neurons

To test neuronal excitability we generated action potentials in cultured tDRG neurons from WT and RAGE KO mice, mantained in either in control or LPS conditions. We quantified action potentials generated by the injection of depolarizing current steps (0 to 1000 pA, at 100pA increments; Fig. 3.4). Cultured tDRG neurons from WT mice treated with LPS displayed a significant (p<0.05) increase in mean action potential counts at 200pA (5.08 ± 0.96 counts) compared to controls (2.42 ± 0.56 counts; Fig. 3.4A, B). In contrast, there were no significant (p>0.05) differences in action potential counts between the control (2.63 ± 0.60 counts) and LPS groups (2.45 ± 0.58 counts) in tDRG neurons from RAGE KO mice (Fig. 3.4A, C). There were no significant differences (p>0.05) in mean resting membrane potentials in WT and RAGE KO tDRG neurons under control and inflammatory conditions (Table 3.1).

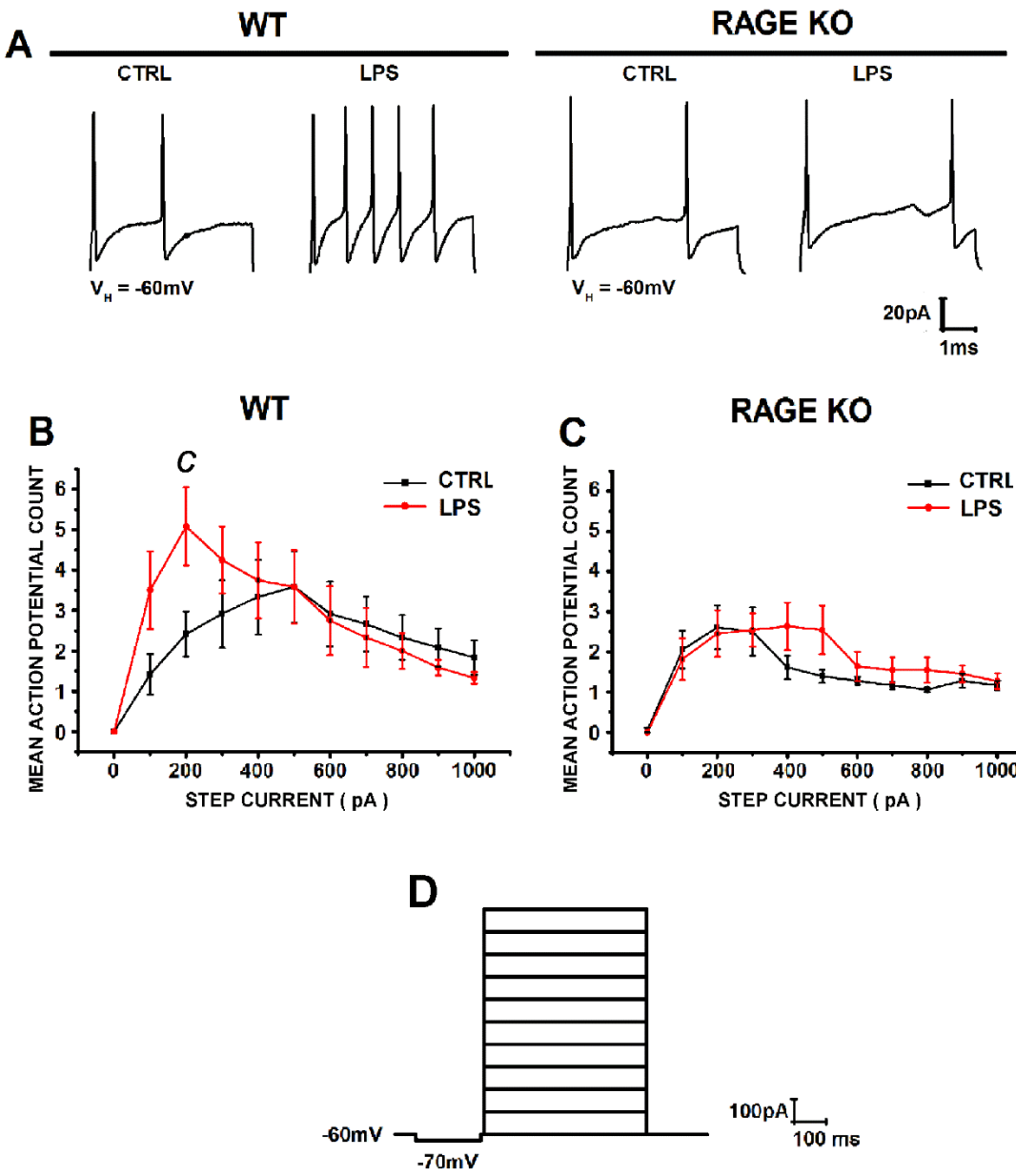

Figure 3.4 LPS exposure increases cell excitability in DRG neurons from WT mice. (A) Representative action potential traces in response to injection of depolarizing current steps (0 to 1000 pA, at 200 pA increments). Mean action potential counts generated in tDRG neurons exposed to either control or from **(B)** WT and **(C)** RAGE KO groups (control and LPS). Error bars represent mean ± SEM. Letter '*c*' denotes $p<0.05$ based on Mann-Whitney Test. **(D)** Step current injection protocol used in whole-cell current-clamp electrophysiology experiments. Treatment groups: WT control (12); WT LPS (12); RAGE KO control (16); RAGE KO LPS (11). Control group is abbreviated as 'CTRL'.

TREATMENT GROUP					
	WT CTRL	**WT LPS**	**WT CC**	**RAGE KO CTRL**	**RAGE KO LPS**
Mean V_{RM} ± SEM (mV)	-44.65 ± 2.43	-48.20 ± 2.32	-44.37 ± 2.25	-47.28 ± 1.56	-47.66 ± 1.88

Table 3.1 Mean V_{RM} of WT and RAGE KO tDRG neurons under control and inflammatory conditions. Combined mean resting membrane potential of WT and RAGE KO experimental groups recorded in voltage- (excluding dose-response experiments) and current-clamp experiments. Treatment groups: WT CTRL (25); WT LPS (21); WT CC (10); RAGE KO CTRL (24) and RAGE KO LPS (20). Raw values from each treatment group were compared using the Kruskal-Wallis Test (non-parametric ANOVA) and found to be not significantly different (p>0.05). Control group is abbreviated as 'CTRL'.

3.5 Expression profile of RAGE and its isoforms in tDRG neurons exposed to LPS

In this study, we detected an increase in expression levels of full length RAGE (Tv1-RAGE; 41.1 arbitrary units, a.u.) in tDRG neurons from WT mice exposed to LPS, with respect to control (26.3 a.u.) (Fig 3.5). Next, I investigated the expression of specific RAGE isoforms under different experimental conditions. This was done by identifying and mapping specific peptides to regions of the respective RAGE isoforms (Table 3.2). Peptides mapped to the N-terminus of *Mmus*RAGEv1 (membrane-bound) and C-terminus of *Mmus*RAGEv2 (soluble), confirmed the expression of these two RAGE isoforms in tDRG neurons from WT mice. However, other peptides failed to map uniquely to other isoforms, and further bioinformatics analysis will be needed to identify their presence. Therefore, only data for isoforms *Mmus*RAGEv1 and v2, and only those with the highest intensity were included (Fig 3.6A, B). In WT tDRG neurons (Fig. 3.6A) under control conditions, the membrane fraction revealed *Mmus*RAGEv1 and v2 levels to be 0.10 a.u. and 2.03 a.u., respectively. In the membrane fraction of LPS-treated neurons, *Mmus*RAGEv1 was not detected and *Mmus*RAGEv2 decreased (0.75 a.u.) relative to controls. In the cytosolic fraction, 5.38 a.u. *Mmus*RAGEv1 was detected in control, and no *Mmus*RAGEv2 was detected. The cytosolic fraction of LPS-treated neurons showed a decrease in *Mmus*RAGEv1 (2.74 a.u.) and an increase in *Mmus*RAGEv2 (1.35 a.u.), relative to controls. In addition, peptides mapped to the *Mmus*RAGEv1 and v2 revealed posttranslational modifications (Figure 3.6B). Our findings show that Thr5 (threonine 5 residue) of *Mmus*RAGEv1 was phosphorylated in the membrane fractions while Thr12 (threonine 12 residue) was found to be phosphorylated in the cytosolic fraction. Additionally, in the cytosolic fraction, Ser307 (serine 307 residue) of *Mmus*RAGEv2 was found to be phosphorylated.

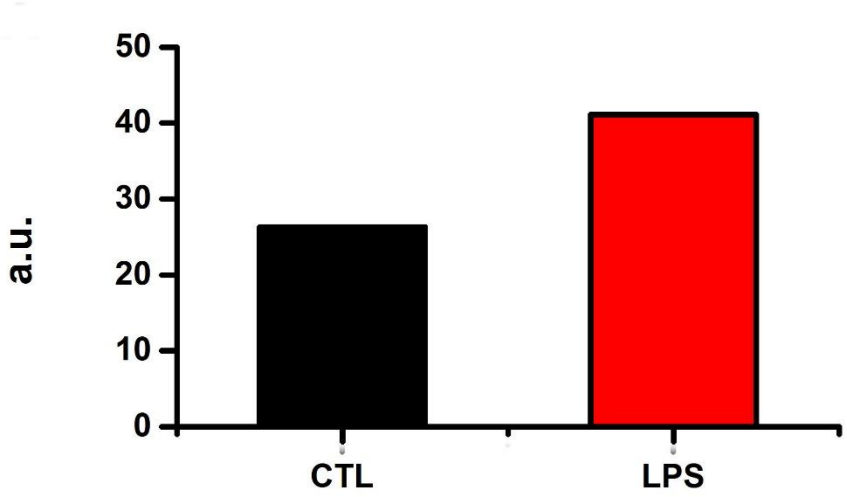

Figure 3.5 MS-based identification of peptide signal intensities of full length RAGE (Tv1-RAGE). Data were collected from cultured tDRG neurons from WT mice exposed to control and LPS conditions. Arbitrary Unit is abbreviated '*a.u.*'.

A

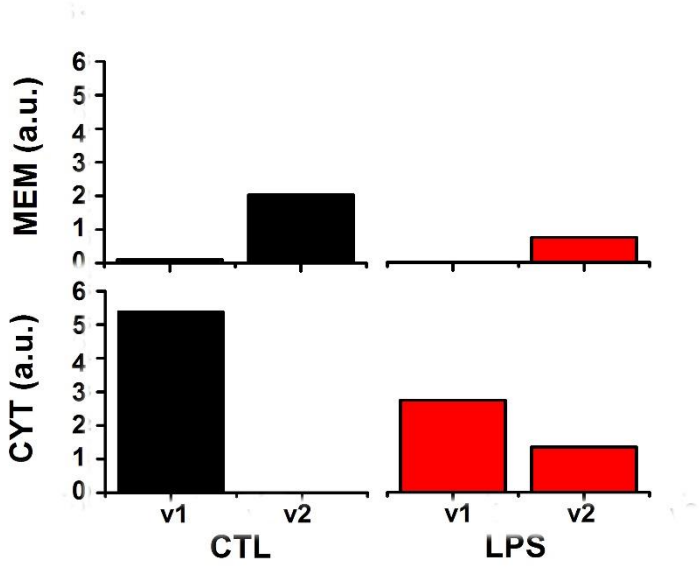

B

Accession #	WT MEM CTL	WT MEM CTL	Modifications	Total Intensity	Total Intensity ($x10^6$)
322718476	isoform 1	mETAtGIVDEGTFR (N-terminal)	m:Oxidized methionine t:Phosphorylated T	98700	0.10
322718478	isoform 2	ALWVSLGWVR (C-terminal)	none	2030000	2.03

Accession #	WT MEM LPS	WT MEM LPS	Modifications	Total Intensity	Total Intensity ($x10^6$)
322718476	isoform 1	Not detected	-	-	-
322718478	Isoform 2	ALWVSLGWVR (C-terminal)	none	746000	0.75

Accession #	WT CYT CTL	WT CYT CTL	Modifications	Total Intensity	Total Intensity ($x10^6$)
322718476	isoform 1	mETATGIVDEGtFR (N-terminal)	m:Oxidized methionine t:Phosphorylated T	5380000	5.38
322718478	isoform 2	Not detected	-	-	-

Accession #	WT CYT LPS	WT CYT LPS	Modifications	Total Intensity	Total Intensity ($x10^6$)
322718476	isoform 1	mETATGIVDEGtFR (N-terminal)	m:Oxidized methionine t:Phosphorylated T	2740000	2.74
322718478	isoform 2	GQLKALWVsLGWVR (C-terminal)	s:Phosphorylated S	1345500	1.35

Figure 3.6 MS-based peptide identification of RAGE isoforms 1-2 (*Mmus*RAGEv1-2 abbreviated as 'v1' and 'v2', respectively). (A) Bar graph membrane and cytosolic fractions of *Mmus*RAGEv1 and v2 under control and LPS-treated conditions in WT tDRGs from neonatal mice. Top row indicates control and LPS membrane fractions. Bottom row indicates control and LPS cytosolic fractions. Arbitrary Unit is abbreviated '*a.u.*'. (B) Total intensities of unique RAGE isoform peptides identified by MS-based proteomics from WT tDRGs.

CHAPTER 4
DISCUSSION & CONCLUSION

Parasympathetic (vagal) and sympathetic (DRG) sensory afferents are known to trigger protective reflexes in the upper airways in response to particulate matter and chemical irritants. Under chronic inflammatory conditions, these systems have been proposed to become hyperactive and contribute to the overproduction of ASL by SGs in the upper airways. At a later stage, airway tissues undergo remodelling which drastically worsens mucociliary clearance and enhances bacterial colonization. Protective reflex responses in the upper airways have been mostly studied as the result of activation of the vagal parasympathetic branch innervating the airways (Bessac and Jordt, 2008; Kollarik et al., 2010). In contrast, much less is known about the role of sympathetic afferent DRG neurons in these reflex responses. In my research, I studied the sensitization of sympathetic afferent tDRG neurons, which innervate SGs in the upper airways (Ianowski et al., 2007; Rogers, 2001; Wine, 2007). LPS exposure caused sensitization of cultured tDRG neurons, manifested as potentiation of CAP-evoked currents and increased action potential generation. These effects require RAGE, and the LPS treatment failed to induce sensitization of tDRG neurons from RAGE KO mice (Myint et al., 2006). LPS-induced sensitization of tDRG neurons correlates with changes in the expression pattern and posttranslational modifications of at least two RAGE isoforms, *Mmus*RAGEv1 and v2 (Lopez-Diez et al., 2013).

4.1 LPS-mediated sensitization of tDRG neurons

In the current study, I concentrated on TRPV1-evoked currents, together with evoked action potentials, as a tool to monitor excitability in tDRG neurons. TRPV1 sensory transduction plays a

major role in sensory signaling in the airways, being expressed in sympathetic (DRG) and parasympathetic (vagal) afferents, and contributing not only to nociception but also to the initiation of protective reflexes as cough and mucus secretion in response to irritants (Lee and Yu, 2014). Here, I investigated the effect of LPS on tDRG neurons known to innervate the upper airways. My data revealed that LPS treatment induced the potentiation of TRPV1-evoked currents and increased action potential firing in tDRG neurons from wild type mice, where neither of these effects were based on changes in resting potential. In contrast, LPS failed to induce these sensitization-related changes in tDRG neurons from RAGE KO mice. The lack of effect of LPS on neurons from RAGE KO mice suggests that either LPS leads to the expression/production of inflammatory mediators that rely on RAGE signalling, or that LPS itself triggers RAGE activation. The latter is consistent with the report by Yamamoto et al. (2011) showing that LPS can bind to RAGE. LPS is known to act through TLR4 receptors, however, our results suggest that in tDRG neurons from RAGE KO mice this pathway may not be active. In fact, it has been recently suggested that RAGE and TLRs can cooperate to produce an inflammatory response to some shared ligands, such as HMGB1 (Ibrahim et al., 2013). It was previously reported that when TLR4, which usually co-localizes with TRPV1 in sensory neurons, is activated by LPS it sensitizes TRPV1, resulting in increased pain signaling (Diogenes et al., 2011; Li et al., 2015a). My data suggest that RAGE may be required for this effect to take place in tDRG neurons. Activation of TLR4 and RAGE lead to shared downstream signaling pathways involving activation of adapter proteins MYD88 (myeloid differentiation primary response 88)-NF-κB and MAPK signaling cascades (Li et al., 2015b; Yu et al., 2011) supporting my findings of required cooperation or co-activation of these receptors in tDRG neurons.

My study revealed that expression of RAGE during LPS treatment is required for TRPV1 potentiation and increased excitability of tDRG neurons. It is well accepted that the interaction of RAGE with its ligands leads to the production of cytosolic ROS (Ott et al., 2014; Vincent et al., 2007), which has been particularly studied in the context of diabetes and arteriosclerosis (Coughlan et al., 2009; Giacco and Brownlee, 2010). In addition, cytosolic ROS have been shown to potentiate CAP-evoked currents by cysteine modification of the TRPV1 channels recovering the receptor from agonist-induced desensitization, which was postulated as an underlying mechanisms of pain abnormalities (Chuang and Lin, 2009). Thus, tDRG neuron sensitization during LPS exposure could be linked to RAGE-induced oxidative stress. A comparison of TRPV1-evoked currents in tDRG neurons from WT vs RAGE KO mice showed similar sensitivity to CAP, as the EC_{50} were not significant different. However, neurons from RAGE KO mice had significantly smaller peak amplitudes (as well as current density and charge) with respect to those of neurons from WT mice at 1, 2.5 and 5 µM CAP. Although, it is unclear at this point the bases of this difference, a report from our lab has shown that autonomic neurons from RAGE KO mice have lower basal ROS levels than neurons from WT mice (Chandna et al., 2015), which may contribute to smaller TRPV1-evoked currents. In addition, it has been reported that TRPV1 channels require proto-oncogene tyrosine-protein kinase (Src) function in colonic DRG neurons (Jin et al., 2004), therefore, considering that Src is a kinase downstream from RAGE (Sorci et al., 2010), it is possible that lack of RAGE expression may have an effect on the basal activity of the TRPV1 channels. In addition, the basal sensitivity of TRPV1 to chemicals and toxins is thought to be modulated by protein kinase C beta type II (PKCβII). RAGE-dependent activation of PKCβII allows for the phosphorylation of TRPV1 channels thus increasing its activity and consequent sensitization (Mandadi et al., 2011).

In the current study we showed that RAGE is required for the increase in neuronal excitability during LPS exposure. Previously reported experiments involving LPS-treated colonic mouse DRGs also showed increased action potential spiking (Ochoa-Cortes et al., 2010). Inflammation at the level of the peripheral terminal is thought to increase action potential spiking through changes in voltage-gated sodium channels, potassium channels, chloride inward rectifier and calcium channels, however, sodium and potassium channels have been regarded with higher importance to this effect. NaV1.8 has been attributed to repetitive firing in DRGs, specifically because of its rapid repriming kinetics. Knockout models of NaV1.8 showed normal responses to noxious stimuli but exhibited blunted visceral sensitization after topical application of irritants (Beyak and Vanner, 2005). RAGE may modulate membrane depolarization through NaV1.8 (voltage-gated sodium channel subtype 1.8) (Gold and Gebhart, 2010), however, the potential link between NaV1.8 and RAGE remains to be addressed. In addition to voltage-gated sodium channels, Kv1.4 and 4.2 among other expressed potassium channels are believed to play a role in regulating excitability through the modulation of the activation threshold and/or firing rate or sustained action potential discharge. These channels have been shown to co-localize with DRGs that express TRPV1 and CGRP and appear to influence transient I_A type currents. In a model of visceral inflammation, a reduction in peak I_A current resulted in a hyperpolarizing shift in the inactivation curve, indicative of less I_A contributing channels available at or near the resting membrane potential (Beyak and Vanner, 2005).

Lipid raft clustering is a long standing phenomena of chronic inflammation, sepsis and various other diseases. Lipid rafts, composed of sphingolipids and cholesterol, are dynamic assemblies of proteins and lipids that float freely within the lipid bilayer of the cell membrane. Ligand binding or oligomerization can cluster or disrupt proteins in or out of rafts. Moreover,

certain ligand-activated proteins display increased raft affinity which then initiate downstream signalling cascades (Simons and Ehehalt, 2002). One study showed that the binding of AGEs to RAGE can increase its trafficking to lipid rafts (Munesue et al., 2013). Coincidentally, cholesterol depletion by methyl β-cyclodextrin (mβCD) of TRPV1-containing lipid rafts exhibited reduced Ca^{2+} influx in rat trigeminal sensory neurons following CAP exposure (Szoke et al., 2010). Similar outcomes were observed in another study where neuronal excitability was diminished in NaV1.8-containing lipid rafts of rat DRG neurons that were dissociated with mβCD treatment (Pristerà et al., 2012). These evidences point to the possibility that RAGE activation may increase its affinity and trafficking to clustered TRPV1- and NaV1.8-contaning lipid rafts that result in increased Ca^{2+} uptake and neuronal excitability. To ascertain if this is due to gene regulation or the inhibition of translocation to the cell surface, transcription and expression analyses would need to be performed in future experiments.

4.2 Expression of RAGE and its isoforms in tDRG neurons

Data gathered from the MS analysis identified changes in levels of RAGE and some of its isoforms in tDRG neurons from WT mice exposed to LPS. Expression levels of full length RAGE (Tv1-RAGE) is expected to increase under inflammatory conditions (Chakraborty et al., 2013; Li et al., 2014), however changes in the expression patterns of RAGE isoforms has not been previously explored. From the 17 alternative splice isoforms of RAGE described in mice, two isoforms were identified in tDRG, *Mmus*RAGEv1 and v2 (Lopez-Diez et al., 2013). Both isoforms contain the first two Ig domains, IgV and IgC2-1 and -2, which form the ligand binding site of the receptor. As described by Lopez-Diez et al. (2013), isoform *Mmus*RAGEv1 lacks exon 1, including the signal peptide region, and parts of exons 2 and 3, but the rest of the transcript is unaltered including

the membrane domain. The detection of *Mmus*RAGEv1 in tDRG samples was surprising, first of all, our samples were collected at postnatal days 1-4 and this particular isoform was only found before in 11 day old embryonic mice and was not detected in later embryonic stages. The latter, is intriguing and may suggest that this protein is expressed in postnatal life. In fact, our MS data analyses of posttranslational changes revealed phosphorylation changes in *Mmus*RAGEv1, these modifications have not been investigated before and may be associated to changes in the proteome that occurs in postnatal life. Second, the transcript for *Mmus*RAGEv1 lacks the signal peptide region, which indicates that the translated protein will not be able to enter the intracellular vesicular transport system at the endoplasmic reticulum, and therefore, will not insert into the plasma membrane (Boron and Boulpaep, 2008). Perhaps this is the reason why we observed higher levels of this protein in the cytosol versus membrane, still the presence of a membrane domain is puzzling and further studies need to be conducted to better understand the expression and role of this isoform. *Mmus*RAGEv2 (Lopez-Diez et al., 2013), which contains the signal peptide domain and the first two Ig domains, and a stop codon before exon 10, could generate soluble versions of RAGE. The generation of RAGE soluble protein versions have been discussed before, Harashima et al. (2006) addressed this possibility by intron 9 retention, and Kang et al. (2014) revealed the role of soluble intracellular RAGE isoforms participating downstream of the extracellular signal–regulated kinases (ERK) in pancreatic cancer cells. The detection of this isoform in tDRG neurons is particularly interesting, since its increase in the cytosolic fraction after LPS treatment is consistent with possible cytosolic signalling, as shown in pancreatic cancer cells (Kang et al., 2014). Furthermore, the expression of *Mmus*RAGEv2 in the cytosolic fraction after LPS treatment shows phosphorylation in amino acid residue serine 307 (Ser 307), which is reminiscent of the serine phosphorylation site identified in full length RAGE (amino acid residue serine 377; Ser

377). In pancreatic cancer cells, Ser377 is a particularly important site that undergoes phosphorylation by ERK1/2 (extracellular signal–regulated kinases 1 and 2), phosphorylated RAGE is been proposed to accumulate in the mitochondria and modulate ATP biosynthesis (Kang et al., 2014). Thus, a serine phosphorylation site in the vicinity of Ser 377 opens new questions of modulation of this isoform that will be addressed in future experiments. At this point, we cannot explain the detection of *Mmus*RAGEv2 in the membrane fraction of tDRG neuron samples. Since this isoform does not contain a membrane domain, we may be detecting another similar isoform or contamination with the cytosolic fraction.

Different biological processes have been previously reported to remove the transmembrane domain and allow the generation of soluble RAGE (sRAGE), either by alternative splicing (esRAGE; endogenous secretory RAGE) or proteolytic cleavage (Maillard-Lefebvre et al., 2009) of carboxyl-terminal truncation of membrane-bound isoforms (cRAGE; cleaved RAGE) (Hanford et al., 2004) by the sheddase ADAM10 (a disintegrin and metalloproteinase domain-containing protein 10) (Raucci et al., 2008). The functional association of *Mmus*RAGEv1 and v2 to neurogenic inflammation are unknown as this is the first study to identify the isoforms in sympathetic afferent tDRG neurons. Most of these isoforms have no physiological function yet. Although preliminary, it is interesting to note that *Mmus*RAGEv2 was detected in the tDRG membrane fraction, without any changes after LPS treatment. We cannot explain this observation at this point, however, this suggests further studies are required to look for residual expression of potential cytosolic RAGE isoforms in the RAGE KO mouse.

4.3 Challenges

This work has established RAGE as a key mediator in LPS-induced sensitization of afferent tDRG neurons of the upper airway in mice. This was demonstrated from electrophysiological data showing the failure of LPS to potentiate CAP-evoked TRPV1 currents and increase action potential generation in RAGE KO relative to WT tDRG neurons. MS analysis for protein identification represents a step forward in biochemistry, allowing to obtain a global picture of the proteins expressed in a cell, including isoforms, post-translational modifications and downstream signalling pathways. However, MS also presents multiple limitations and pitfalls, many of which were evident during my study. The main reasons why we decided to explore MS as a protein identification technique for the expression of RAGE and its isoforms was due to the lack of commercially available antibodies for RAGE isoforms and the interest of exploring post-translational modifications. However, as reviewed by Lubec and Afjehi-Sadat (2007), multiple factors can hamper the power of MS, such as the low abundance of protein in the samples tested and the complexity of bioinformatic analysis. The expression level of RAGE isoforms (detected and not detected) vary significantly among tests, which was likely due to the low abundance of protein. In addition, we may have been "blind" to changes in expression levels of RAGE isoforms that were not detected by the used MS analysis. The major limiting factor here was the ability to obtain high cell numbers given that this study employed primary and not immortalized cell cultures. The latter forced us to combined samples collected over a period of 5 months and to perform sensitive steps multiple times increasing our chances of cross-contamination. Thus, we were not only faced with very low protein concentrations but also we encountered intriguing results, such as detecting a cytosolic version of RAGE in the membrane fractions. To confirm the findings of this study, qPCR could be performed to not only evaluate the presence and expression

of *Mmus*RAGEv1 and v2, but other RAGE isoforms that may be present in tDRGs and undetected by MS analysis. The results presented in this thesis were generated as a preliminary analysis of the vast amount of data obtained by MS of tDRG neurons exposed to either control or LPS treatment. This was the stepping stone that triggered follow up experiments that are currently underway to explore the full potential of our samples. Unfortunately, the latter escapes the scope of this thesis and have not been included. Thus, the pitfalls listed here, although have affected and limited the findings included in this thesis, have also helped us to better design and to optimize the MS analysis of the tDRG samples.

4.4 Conclusions and Future Directions

Given the complexity of neurogenic inflammation and the multi-ligand promiscuity of RAGE, further examination of RAGE will need to be done to confirm its interaction (direct or indirect) with LPS *in vivo* and *in vitro*. This is because it is known that other PRRs such as TLR4 do interact with LPS. As yet, there is no compelling evidence to suggest that LPS binds to RAGE *in vitro* or *in vivo* in sympathetic afferent tDRGs. Although the purpose of this thesis was not to explore the interaction of LPS with RAGE or its cascade of mechanisms, the magnitude of response from this interaction should be assessed in WT tDRGs with RAGE and TLR4 antagonists. This would help confirm the cognate experiments done using RAGE KO tDRGs. The caveat with using a knock-out model such as the tDRG neurons from RAGE KO mice is that its tissues are biochemically different. For instance, RAGE KO peripheral neurons inherently have markedly lower redox states under control conditions and such differences may offset responses from LPS-induced sensitization.

MS analyses have identified isoforms *Mmus*RAGEv1-2 in afferent tDRG neurons following LPS treatment. To this effect, siRNA (small interfering RNA) could be designed to strategically block the expression of these isoforms before and after LPS exposure in WT tDRGs. Calcium imaging to reflect neuronal excitability and electrophysiological experiments to assess CAP-evoked TRPV1 potentiation and action potential generation can be studied. Information gathered from these *in vitro* experiments could be extended to *ex vivo* studies using mouse airway explants to study the contribution of tDRG to mucus secretion. Mouse tracheal explants could be treated with powdered siRNA (Lam et al., 2012) and observed for changes to ASL levels by *in situ* recording of airway plexuses.

In vivo experiments manipulating the expression of specific RAGE isoforms by powdered siRNA could potentially be used to treat live mice that have been exposed to LPS and their tissues assessed for biochemical and other changes. For example, brochoalveolar lavage and tissue samples can be obtained and assessed for gross morphological changes, leukocyte counts and airway diameter clearance. Mice tracheal explants could also be used to study secretion rates and ASL levels. Additionally, MS analysis revealed changes in the expression of two RAGE isoforms in WT tDRGs treated with LPS. These isoforms would now require further examination and could potentially serve as a targeted strategy in RAGE-associated airway inflammatory diseases.

REFERENCES

Alexander, C., Rietschel, E.T., 2001. Bacterial lipopolysaccharides and innate immunity. J Endotoxin Res 7, 167-202.

Allette, Y.M., Due, M.R., Wilson, S.M., Feldman, P., Ripsch, M.S., Khanna, R., White, F.A., 2014. Identification of a functional interaction of HMGB1 with Receptor for Advanced Glycation End-products in a model of neuropathic pain. Brain Behav Immun 42, 169-177.

Ansel, J.C., Brown, J.R., Payan, D.G., Brown, M.A., 1993. Substance P selectively activates TNF-alpha gene expression in murine mast cells. J Immunol 150, 4478-4485.

Barnes, P.J., 2001. Neurogenic inflammation in the airways. Respir Physiol 125, 145-154.

Barnes, P.J., Rodger, I.W., Thomson, N.C., 1998. Asthma, basic mechanisms and clinical management, 3rd ed. Academic Press, San Diego.

Bautista, D.M., Jordt, S.E., Nikai, T., Tsuruda, P.R., Read, A.J., Poblete, J., Yamoah, E.N., Basbaum, A.I., Julius, D., 2006. TRPA1 mediates the inflammatory actions of environmental irritants and proalgesic agents. Cell 124, 1269-1282.

Bayliss, W.M., 1901. On the origin from the spinal cord of the vaso-dilator fibres of the hind-limb, and on the nature of these fibres. J Physiol 26, 173-209.

Bessac, B.F., Jordt, S.E., 2008. Breathtaking TRP channels: TRPA1 and TRPV1 in airway chemosensation and reflex control. Physiology (Bethesda) 23, 360-370.

Beyak, M.J., Vanner, S., 2005. Inflammation-induced hyperexcitability of nociceptive gastrointestinal DRG neurones: the role of voltage-gated ion channels. Neurogastroenterol Motil 17, 175-186.

Boron, W.F., Boulpaep, E.L., 2008. Medical Physiology. Elsevier Health Sciences.

Bowden, J.J., Gibbins, I.L., 1992. Vasoactive intestinal peptide and neuropeptide Y coexist in non-noradrenergic sympathetic neurons to guinea pig trachea. J Auton Nerv Syst 38, 1-19.

Brain, S.D., Williams, T.J., 1989. Interactions between the tachykinins and calcitonin gene-related peptide lead to the modulation of oedema formation and blood flow in rat skin. Br J Pharmacol 97, 77-82.

Buckley, S.T., Ehrhardt, C., 2010. The receptor for advanced glycation end products (RAGE) and the lung. J Biomed Biotechnol 2010, 917108.

Caceres, A.I., Brackmann, M., Elia, M.D., Bessac, B.F., del Camino, D., D'Amours, M., Witek, J.S., Fanger, C.M., Chong, J.A., Hayward, N.J., Homer, R.J., Cohn, L., Huang, X., Moran, M.M., Jordt, S.E., 2009. A sensory neuronal ion channel essential for airway inflammation and hyperreactivity in asthma. Proc Natl Acad Sci U S A 106, 9099-9104.

Campanucci, V.A., Krishnaswamy, A., Cooper, E., 2008. Mitochondrial reactive oxygen species inactivate neuronal nicotinic acetylcholine receptors and induce long-term depression of fast nicotinic synaptic transmission. J Neurosci 28, 1733-1744.

Chakraborty, R., Bhatt, K.H., Sodhi, A., 2013. High mobility group box 1 protein synergizes with lipopolysaccharide and peptidoglycan for nitric oxide production in mouse peritoneal macrophages in vitro. Mol Immunol 54, 48-57.

Chandna, A.R., Nair, M., Chang, C., Pennington, P.R., Yamamoto, Y., Mousseau, D.D., Campanucci, V.A., 2015. RAGE mediates the inactivation of nAChRs in sympathetic neurons under high glucose conditions. Eur J Neurosci 41, 341-351.

Chiu, I.M., von Hehn, C.A., Woolf, C.J., 2012. Neurogenic inflammation and the peripheral nervous system in host defense and immunopathology. Nat Neurosci 15, 1063-1067.

Chuang, H.H., Lin, S., 2009. Oxidative challenges sensitize the capsaicin receptor by covalent cysteine modification. Proc Natl Acad Sci U S A 106, 20097-20102.

Coughlan, M.T., Thorburn, D.R., Penfold, S.A., Laskowski, A., Harcourt, B.E., Sourris, K.C., Tan, A.L., Fukami, K., Thallas-Bonke, V., Nawroth, P.P., Brownlee, M., Bierhaus, A., Cooper, M.E., Forbes, J.M., 2009. RAGE-induced cytosolic ROS promote mitochondrial superoxide generation in diabetes. J Am Soc Nephrol 20, 742-752.

Cyphert, J.M., Kovarova, M., Allen, I.C., Hartney, J.M., Murphy, D.L., Wess, J., Koller, B.H., 2009. Cooperation between mast cells and neurons is essential for antigen-mediated bronchoconstriction. J Immunol 182, 7430-7439.

de Groat, W.C., Yoshimura, N., 2009. Afferent nerve regulation of bladder function in health and disease. Handb Exp Pharmacol, 91-138.

Ding, W., Stohl, L.L., Wagner, J.A., Granstein, R.D., 2008. Calcitonin gene-related peptide biases Langerhans cells toward Th2-type immunity. J Immunol 181, 6020-6026.

Dinh, Q.T., Groneberg, D.A., Peiser, C., Mingomataj, E., Joachim, R.A., Witt, C., Arck, P.C., Klapp, B.F., Fischer, A., 2004. Substance P expression in TRPV1 and trkA-positive dorsal root ganglion neurons innervating the mouse lung. Respir Physiol Neurobiol 144, 15-24.

Diogenes, A., Ferraz, C.C., Akopian, A.N., Henry, M.A., Hargreaves, K.M., 2011. LPS sensitizes TRPV1 via activation of TLR4 in trigeminal sensory neurons. J Dent Res 90, 759-764.

Dong, F., Du, Y.R., Xie, W., Strong, J.A., He, X.J., Zhang, J.M., 2012. Increased function of the TRPV1 channel in small sensory neurons after local inflammation or in vitro exposure to the pro-inflammatory cytokine GRO/KC. Neurosci Bull 28, 155-164.

Edvinsson, L., Ekman, R., Jansen, I., McCulloch, J., Uddman, R., 1987. Calcitonin gene-related peptide and cerebral blood vessels: distribution and vasomotor effects. J Cereb Blood Flow Metab 7, 720-728.

Engel, M.A., Leffler, A., Niedermirtl, F., Babes, A., Zimmermann, K., Filipovic, M.R., Izydorczyk, I., Eberhardt, M., Kichko, T.I., Mueller-Tribbensee, S.M., Khalil, M., Siklosi, N., Nau, C., Ivanovic-Burmazovic, I., Neuhuber, W.L., Becker, C., Neurath, M.F., Reeh, P.W., 2011. TRPA1 and substance P mediate colitis in mice. Gastroenterology 141, 1346-1358.

Fischer, A.J., Goss, K.L., Scheetz, T.E., Wohlford-Lenane, C.L., Snyder, J.M., McCray, P.B., Jr., 2009. Differential gene expression in human conducting airway surface epithelia and submucosal glands. Am J Respir Cell Mol Biol 40, 189-199.

Fisher, A.W., 1964. The Intrinsic Innervation of the Trachea. J Anat 98, 117-124.

Giacco, F., Brownlee, M., 2010. Oxidative stress and diabetic complications. Circ Res 107, 1058-1070.

Gold, M.S., Gebhart, G.F., 2010. Nociceptor sensitization in pain pathogenesis. Nat Med 16, 1248-1257.

Goldin, A., Beckman, J.A., Schmidt, A.M., Creager, M.A., 2006. Advanced glycation end products: sparking the development of diabetic vascular injury. Circulation 114, 597-605.

Goltz, F., 1874. Über gefässerweiternde Nerven. Pflueger Arch Ges Physiol. 9.

Hall, S.C., Agrawal, D.K., 2015. Toll-like Receptors, Triggering Receptor Expressed on Myeloid Cells Family Members and Receptor for Advanced Glycation End-products in Allergic Airway Inflammation. Expert Rev Respir Med.

Hamid, Q., Shannon, J., Martin, J., 2005. Physiologic basis of respiratory disease. BC Decker, Inc., Hamilton.

Hanford, L.E., Enghild, J.J., Valnickova, Z., Petersen, S.V., Schaefer, L.M., Schaefer, T.M., Reinhart, T.A., Oury, T.D., 2004. Purification and characterization of mouse soluble receptor for advanced glycation end products (sRAGE). J Biol Chem 279, 50019-50024.

Harashima, A., Yamamoto, Y., Cheng, C., Tsuneyama, K., Myint, K.M., Takeuchi, A., Yoshimura, K., Li, H., Watanabe, T., Takasawa, S., Okamoto, H., Yonekura, H., Yamamoto, H., 2006. Identification of mouse orthologue of endogenous secretory receptor for advanced glycation end-products: structure, function and expression. Biochem J 396, 109-115.

Hargreave, F.E., Parameswaran, K., 2006. Asthma, COPD and bronchitis are just components of airway disease. Eur Respir J 28, 264-267.

Hensellek, S., Brell, P., Schaible, H.G., Brauer, R., Segond von Banchet, G., 2007. The cytokine TNFalpha increases the proportion of DRG neurones expressing the TRPV1 receptor via the TNFR1 receptor and ERK activation. Mol Cell Neurosci 36, 381-391.

Hiemstra, P.S., Zaat, S.A.J., 2013. Antimicrobial peptides and innate immunity. Springer, Basel ; New York.

Hofmann, M.A., Drury, S., Fu, C., Qu, W., Taguchi, A., Lu, Y., Avila, C., Kambham, N., Bierhaus, A., Nawroth, P., Neurath, M.F., Slattery, T., Beach, D., McClary, J., Nagashima, M., Morser, J., Stern, D., Schmidt, A.M., 1999. RAGE mediates a novel proinflammatory axis: a central cell surface receptor for S100/calgranulin polypeptides. Cell 97, 889-901.

Hosoi, J., Murphy, G.F., Egan, C.L., Lerner, E.A., Grabbe, S., Asahina, A., Granstein, R.D., 1993. Regulation of Langerhans cell function by nerves containing calcitonin gene-related peptide. Nature 363, 159-163.

Hou, L., Wang, X., 2001. PKC and PKA, but not PKG mediate LPS-induced CGRP release and [Ca(2+)](i) elevation in DRG neurons of neonatal rats. J Neurosci Res 66, 592-600.

Ianowski, J.P., Choi, J.Y., Wine, J.J., Hanrahan, J.W., 2007. Mucus secretion by single tracheal submucosal glands from normal and cystic fibrosis transmembrane conductance regulator knockout mice. J Physiol 580, 301-314.

Ibrahim, Z.A., Armour, C.L., Phipps, S., Sukkar, M.B., 2013. RAGE and TLRs: relatives, friends or neighbours? Mol Immunol 56, 739-744.

Janig, W., Levine, J.D., Michaelis, M., 1996. Interactions of sympathetic and primary afferent neurons following nerve injury and tissue trauma. Prog Brain Res 113, 161-184.

Jin, X., Morsy, N., Winston, J., Pasricha, P.J., Garrett, K., Akbarali, H.I., 2004. Modulation of TRPV1 by nonreceptor tyrosine kinase, c-Src kinase. Am J Physiol Cell Physiol 287, C558-563.

Kang, R., Hou, W., Zhang, Q., Chen, R., Lee, Y.J., Bartlett, D.L., Lotze, M.T., Tang, D., Zeh, H.J., 2014. RAGE is essential for oncogenic KRAS-mediated hypoxic signaling in pancreatic cancer. Cell Death Dis 5, e1480.

Knowles, M.R., Boucher, R.C., 2002. Mucus clearance as a primary innate defense mechanism for mammalian airways. J Clin Invest 109, 571-577.

Kollarik, M., Ru, F., Brozmanova, M., 2010. Vagal afferent nerves with the properties of nociceptors. Auton Neurosci 153, 12-20.

Lam, J.K., Liang, W., Chan, H.K., 2012. Pulmonary delivery of therapeutic siRNA. Adv Drug Deliv Rev 64, 1-15.

Lee, C.C., Lai, Y.T., Chang, H.T., Liao, J.W., Shyu, W.C., Li, C.Y., Wang, C.N., 2013. Inhibition of high-mobility group box 1 in lung reduced airway inflammation and remodeling in a mouse model of chronic asthma. Biochem Pharmacol 86, 940-949.

Lee, L.Y., Yu, J., 2014. Sensory nerves in lung and airways. Compr Physiol 4, 287-324.

Li, Y., Adamek, P., Zhang, H., Tatsui, C.E., Rhines, L.D., Mrozkova, P., Li, Q., Kosturakis, A.K., Cassidy, R.M., Harrison, D.S., Cata, J.P., Sapire, K., Zhang, H., Kennamer-Chapman, R.M., Jawad, A.B., Ghetti, A., Yan, J., Palecek, J., Dougherty, P.M., 2015a. The Cancer Chemotherapeutic Paclitaxel Increases Human and Rodent Sensory Neuron Responses to TRPV1 by Activation of TLR4. J Neurosci 35, 13487-13500.

Li, Y., Wu, R., Tian, Y., Yu, M., Tang, Y., Cheng, H., Tian, Z., 2015b. RAGE/NF-kappaB signaling mediates lipopolysaccharide induced acute lung injury in neonate rat model. Int J Clin Exp Med 8, 13371-13376.

Li, Y., Wu, R., Zhao, S., Cheng, H., Ji, P., Yu, M., Tian, Z., 2014. RAGE/NF-kappaB pathway mediates lipopolysaccharide-induced inflammation in alveolar type I epithelial cells isolated from neonate rats. Inflammation 37, 1623-1629.

Lopez-Diez, R., Rastrojo, A., Villate, O., Aguado, B., 2013. Complex tissue-specific patterns and distribution of multiple RAGE splice variants in different mammals. Genome Biol Evol 5, 2420-2435.

Luan, X., Campanucci, V.A., Nair, M., Yilmaz, O., Belev, G., Machen, T.E., Chapman, D., Ianowski, J.P., 2014. Pseudomonas aeruginosa triggers CFTR-mediated airway surface liquid secretion in swine trachea. Proc Natl Acad Sci U S A 111, 12930-12935.

Lubec, G., Afjehi-Sadat, L., 2007. Limitations and pitfalls in protein identification by mass spectrometry. Chem Rev 107, 3568-3584.

Maggi, C.A., Giachetti, A., Dey, R.D., Said, S.I., 1995. Neuropeptides as regulators of airway function: vasoactive intestinal peptide and the tachykinins. Physiol Rev 75, 277-322.

Maillard-Lefebvre, H., Boulanger, E., Daroux, M., Gaxatte, C., Hudson, B.I., Lambert, M., 2009. Soluble receptor for advanced glycation end products: a new biomarker in diagnosis and prognosis of chronic inflammatory diseases. Rheumatology (Oxford) 48, 1190-1196.

Mandadi, S., Armati, P.J., Roufogalis, B.D., 2011. Real-Time Translocation and Function of PKCβII Isoform in Response to Nociceptive Signaling via the TRPV1 Pain Receptor. Pharmaceuticals 4, 1503.

McCormack, D.G., Mak, J.C., Coupe, M.O., Barnes, P.J., 1989. Calcitonin gene-related peptide vasodilation of human pulmonary vessels. J Appl Physiol (1985) 67, 1265-1270.

McGovern, A.E., Mazzone, S.B., 2014. Neural regulation of inflammation in the airways and lungs. Auton Neurosci 182, 95-101.

Mikami, N., Matsushita, H., Kato, T., Kawasaki, R., Sawazaki, T., Kishimoto, T., Ogitani, Y., Watanabe, K., Miyagi, Y., Sueda, K., Fukada, S., Yamamoto, H., Tsujikawa, K., 2011. Calcitonin gene-related peptide is an important regulator of cutaneous immunity: effect on dendritic cell and T cell functions. J Immunol 186, 6886-6893.

Millqvist, E., 2000. Cough provocation with capsaicin is an objective way to test sensory hyperreactivity in patients with asthma-like symptoms. Allergy 55, 546-550.

Milutinovic, P.S., Alcorn, J.F., Englert, J.M., Crum, L.T., Oury, T.D., 2012. The receptor for advanced glycation end products is a central mediator of asthma pathogenesis. Am J Pathol 181, 1215-1225.

Mulrennan, S., Baltic, S., Aggarwal, S., Wood, J., Miranda, A., Frost, F., Kaye, J., Thompson, P.J., 2015. The Role of Receptor for Advanced Glycation End Products in Airway Inflammation in CF and CF related Diabetes. Sci Rep 5, 8931.

Munesue, S., Yamamoto, Y., Urushihara, R., Inomata, K., Saito, H., Motoyoshi, S., Watanabe, T., Yonekura, H., Yamamoto, H., 2013. Low-molecular weight fractions of Japanese soy sauce act as a RAGE antagonist via inhibition of RAGE trafficking to lipid rafts. Food Funct 4, 1835-1842.

Murata, Y., Rydevik, B., Nannmark, U., Larsson, K., Takahashi, K., Kato, Y., Olmarker, K., 2011. Local application of interleukin-6 to the dorsal root ganglion induces tumor necrosis factor-alpha in the dorsal root ganglion and results in apoptosis of the dorsal root ganglion cells. Spine (Phila Pa 1976) 36, 926-932.

Myint, K.M., Yamamoto, Y., Doi, T., Kato, I., Harashima, A., Yonekura, H., Watanabe, T., Shinohara, H., Takeuchi, M., Tsuneyama, K., Hashimoto, N., Asano, M., Takasawa, S., Okamoto, H., Yamamoto, H., 2006. RAGE control of diabetic nephropathy in a mouse model: effects of RAGE gene disruption and administration of low-molecular weight heparin. Diabetes 55, 2510-2522.

Neeper, M., Schmidt, A.M., Brett, J., Yan, S.D., Wang, F., Pan, Y.C., Elliston, K., Stern, D., Shaw, A., 1992. Cloning and expression of a cell surface receptor for advanced glycosylation end products of proteins. J Biol Chem 267, 14998-15004.

Ochoa-Cortes, F., Ramos-Lomas, T., Miranda-Morales, M., Spreadbury, I., Ibeakanma, C., Barajas-Lopez, C., Vanner, S., 2010. Bacterial cell products signal to mouse colonic nociceptive dorsal root ganglia neurons. Am J Physiol Gastrointest Liver Physiol 299, G723-732.

Ordovas-Montanes, J., Rakoff-Nahoum, S., Huang, S., Riol-Blanco, L., Barreiro, O., von Andrian, U.H., 2015. The Regulation of Immunological Processes by Peripheral Neurons in Homeostasis and Disease. Trends Immunol 36, 578-604.

Ostrowski, S.M., Belkadi, A., Loyd, C.M., Diaconu, D., Ward, N.L., 2011. Cutaneous denervation of psoriasiform mouse skin improves acanthosis and inflammation in a sensory neuropeptide-dependent manner. J Invest Dermatol 131, 1530-1538.

Ott, C., Jacobs, K., Haucke, E., Navarrete Santos, A., Grune, T., Simm, A., 2014. Role of advanced glycation end products in cellular signaling. Redox Biol 2, 411-429.

Plato, M., Kummer, W., Haberberger, R.V., 2006. Structural and neurochemical comparison of vagal and spinal afferent neurons projecting to the rat lung. Neurosci Lett 395, 215-219.

Pristerà, A., Baker, M.D., Okuse, K., 2012. Association between Tetrodotoxin Resistant Channels and Lipid Rafts Regulates Sensory Neuron Excitability. PLoS ONE 7, e40079.

Qiao, M., Zhang, J., 2014. [Effects of inhaled LPS on inflammation and mucus hypersecretion in the airway of asthmatic mice]. Sichuan Da Xue Xue Bao Yi Xue Ban 45, 432-436.

Qin, C., Foreman, R.D., Farber, J.P., 2007. Characterization of thoracic spinal neurons with noxious convergent inputs from heart and lower airways in rats. Brain Res 1141, 84-91.

Raucci, A., Cugusi, S., Antonelli, A., Barabino, S.M., Monti, L., Bierhaus, A., Reiss, K., Saftig, P., Bianchi, M.E., 2008. A soluble form of the receptor for advanced glycation endproducts (RAGE) is produced by proteolytic cleavage of the membrane-bound form by the sheddase a disintegrin and metalloprotease 10 (ADAM10). FASEB J 22, 3716-3727.

Repapi, E., Sayers, I., Wain, L.V., Burton, P.R., Johnson, T., Obeidat, M., Zhao, J.H., Ramasamy, A., Zhai, G., Vitart, V., Huffman, J.E., Igl, W., Albrecht, E., Deloukas, P., Henderson, J., Granell, R., McArdle, W.L., Rudnicka, A.R., Wellcome Trust Case Control, C., Barroso, I., Loos, R.J., Wareham, N.J., Mustelin, L., Rantanen, T., Surakka, I., Imboden, M., Wichmann, H.E., Grkovic, I., Jankovic, S., Zgaga, L., Hartikainen, A.L., Peltonen, L., Gyllensten, U., Johansson, A., Zaboli, G., Campbell, H., Wild, S.H., Wilson, J.F., Glaser, S., Homuth, G., Volzke, H., Mangino, M., Soranzo, N., Spector, T.D., Polasek, O., Rudan, I., Wright, A.F., Heliovaara, M., Ripatti, S., Pouta, A., Naluai, A.T., Olin, A.C., Toren, K., Cooper, M.N., James, A.L., Palmer, L.J., Hingorani, A.D., Wannamethee, S.G., Whincup, P.H., Smith, G.D., Ebrahim, S., McKeever, T.M., Pavord, I.D., MacLeod, A.K., Morris, A.D., Porteous, D.J., Cooper, C., Dennison, E., Shaheen, S., Karrasch, S., Schnabel, E., Schulz, H., Grallert, H., Bouatia-Naji, N., Delplanque, J., Froguel, P., Blakey, J.D., Team, N.R.S., Britton, J.R., Morris, R.W., Holloway, J.W., Lawlor, D.A., Hui, J., Nyberg, F., Jarvelin, M.R., Jackson, C., Kahonen, M., Kaprio, J., Probst-Hensch, N.M., Koch, B., Hayward, C., Evans, D.M., Elliott, P., Strachan, D.P., Hall, I.P., Tobin, M.D., 2010. Genome-wide association study identifies five loci associated with lung function. Nat Genet 42, 36-44.

Rochlitzer, S., Veres, T.Z., Kuhne, K., Prenzler, F., Pilzner, C., Knothe, S., Winkler, C., Lauenstein, H.D., Willart, M., Hammad, H., Muller, M., Krug, N., Lambrecht, B.N., Braun, A., 2011. The neuropeptide calcitonin gene-related peptide affects allergic airway inflammation by modulating dendritic cell function. Clin Exp Allergy 41, 1609-1621.

Rogers, D.F., 2001. Mucus hypersecretion in chronic obstructive pulmonary disease. Novartis Found Symp 234, 65-77; discussion 77-83.

Rong, L.L., Yan, S.F., Wendt, T., Hans, D., Pachydaki, S., Bucciarelli, L.G., Adebayo, A., Qu, W., Lu, Y., Kostov, K., Lalla, E., Yan, S.D., Gooch, C., Szabolcs, M., Trojaborg, W., Hays, A.P., Schmidt, A.M., 2004. RAGE modulates peripheral nerve regeneration via recruitment of both inflammatory and axonal outgrowth pathways. FASEB J 18, 1818-1825.

Ruderman, N.B., Williamson, J.R., Brownlee, M., 1992. Glucose and diabetic vascular disease. FASEB J 6, 2905-2914.

Ruscheweyh, R., Forsthuber, L., Schoffnegger, D., Sandkuhler, J., 2007. Modification of classical neurochemical markers in identified primary afferent neurons with Abeta-, Adelta-, and C-fibers after chronic constriction injury in mice. J Comp Neurol 502, 325-336.

Saleh, A., Chowdhury, S.K., Smith, D.R., Balakrishnan, S., Tessler, L., Schartner, E., Bilodeau, A., Van Der Ploeg, R., Fernyhough, P., 2013. Diabetes impairs an interleukin-1beta-dependent pathway that enhances neurite outgrowth through JAK/STAT3 modulation of mitochondrial bioenergetics in adult sensory neurons. Mol Brain 6, 45.

Santoni, G., Cardinali, C., Morelli, M.B., Santoni, M., Nabissi, M., Amantini, C., 2015. Danger- and pathogen-associated molecular patterns recognition by pattern-recognition receptors and ion channels of the transient receptor potential family triggers the inflammasome activation in immune cells and sensory neurons. J Neuroinflammation 12, 21.

Saria, A., 1984. Substance P in sensory nerve fibres contributes to the development of oedema in the rat hind paw after thermal injury. Br J Pharmacol 82, 217-222.

Sauer, S.K., Reeh, P.W., Bove, G.M., 2001. Noxious heat-induced CGRP release from rat sciatic nerve axons in vitro. Eur J Neurosci 14, 1203-1208.

Schmidt, A.M., Hasu, M., Popov, D., Zhang, J.H., Chen, J., Yan, S.D., Brett, J., Cao, R., Kuwabara, K., Costache, G., et al., 1994. Receptor for advanced glycation end products (AGEs) has a central role in vessel wall interactions and gene activation in response to circulating AGE proteins. Proc Natl Acad Sci U S A 91, 8807-8811.

Schmidt, A.M., Vianna, M., Gerlach, M., Brett, J., Ryan, J., Kao, J., Esposito, C., Hegarty, H., Hurley, W., Clauss, M., et al., 1992. Isolation and characterization of two binding proteins for advanced glycosylation end products from bovine lung which are present on the endothelial cell surface. J Biol Chem 267, 14987-14997.

Sessa, L., Gatti, E., Zeni, F., Antonelli, A., Catucci, A., Koch, M., Pompilio, G., Fritz, G., Raucci, A., Bianchi, M.E., 2014. The receptor for advanced glycation end-products (RAGE) is only present in mammals, and belongs to a family of cell adhesion molecules (CAMs). PLoS One 9, e86903.

Simons, K., Ehehalt, R., 2002. Cholesterol, lipid rafts, and disease. J Clin Invest 110, 597-603.

Sorci, G., Bianchi, R., Riuzzi, F., Tubaro, C., Arcuri, C., Giambanco, I., Donato, R., 2010. S100B Protein, A Damage-Associated Molecular Pattern Protein in the Brain and Heart, and Beyond. Cardiovasc Psychiatry Neurol 2010.

Sparvero, L.J., Asafu-Adjei, D., Kang, R., Tang, D., Amin, N., Im, J., Rutledge, R., Lin, B., Amoscato, A.A., Zeh, H.J., Lotze, M.T., 2009. RAGE (Receptor for Advanced Glycation Endproducts), RAGE ligands, and their role in cancer and inflammation. J Transl Med 7, 17.

Springall, D.R., Cadieux, A., Oliveira, H., Su, H., Royston, D., Polak, J.M., 1987. Retrograde tracing shows that CGRP-immunoreactive nerves of rat trachea and lung originate from vagal and dorsal root ganglia. J Auton Nerv Syst 20, 155-166.

Srikrishna, G., Freeze, H.H., 2009. Endogenous damage-associated molecular pattern molecules at the crossroads of inflammation and cancer. Neoplasia 11, 615-628.

Sukkar, M.B., Ullah, M.A., Gan, W.J., Wark, P.A., Chung, K.F., Hughes, J.M., Armour, C.L., Phipps, S., 2012. RAGE: a new frontier in chronic airways disease. Br J Pharmacol 167, 1161-1176.

Suto, N., Ikura, K., Sasaki, R., 1993. Expression induced by interleukin-6 of tissue-type transglutaminase in human hepatoblastoma HepG2 cells. J Biol Chem 268, 7469-7473.

Szoke, E., Borzsei, R., Toth, D.M., Lengl, O., Helyes, Z., Sandor, Z., Szolcsanyi, J., 2010. Effect of lipid raft disruption on TRPV1 receptor activation of trigeminal sensory neurons and transfected cell line. Eur J Pharmacol 628, 67-74.

Talbot, S., Foster, S.L., Woolf, C.J., 2016. Neuroimmunity: Physiology and Pathology. Annu Rev Immunol 34, 421-447.

Taniguchi, A., Miyahara, N., Waseda, K., Kurimoto, E., Fujii, U., Tanimoto, Y., Kataoka, M., Yamamoto, Y., Gelfand, E.W., Yamamoto, H., Tanimoto, M., Kanehiro, A., 2015. Contrasting roles for the receptor for advanced glycation end-products on structural cells in allergic airway inflammation vs. airway hyperresponsiveness. Am J Physiol Lung Cell Mol Physiol 309, L789-800.

Tobon-Velasco, J.C., Cuevas, E., Torres-Ramos, M.A., 2014. Receptor for AGEs (RAGE) as mediator of NF-kB pathway activation in neuroinflammation and oxidative stress. CNS Neurol Disord Drug Targets 13, 1615-1626.

Todd, A.J., 2010. Neuronal circuitry for pain processing in the dorsal horn. Nat Rev Neurosci 11, 823-836.

Toward, T.J., Broadley, K.J., 2002. Goblet cell hyperplasia, airway function, and leukocyte infiltration after chronic lipopolysaccharide exposure in conscious Guinea pigs: effects of rolipram and dexamethasone. J Pharmacol Exp Ther 302, 814-821.

Truett, G.E., Heeger, P., Mynatt, R.L., Truett, A.A., Walker, J.A., Warman, M.L., 2000. Preparation of PCR-quality mouse genomic DNA with hot sodium hydroxide and tris (HotSHOT). Biotechniques 29, 52, 54.

Tse, K.H., Chow, K.B., Leung, W.K., Wong, Y.H., Wise, H., 2014. Lipopolysaccharide differentially modulates expression of cytokines and cyclooxygenases in dorsal root ganglion cells via Toll-like receptor-4 dependent pathways. Neuroscience 267, 241-251.

Undem, B.J., Carr, M.J., 2002. The role of nerves in asthma. Curr Allergy Asthma Rep 2, 159-165.

Vernooy, J.H., Dentener, M.A., van Suylen, R.J., Buurman, W.A., Wouters, E.F., 2002. Long-term intratracheal lipopolysaccharide exposure in mice results in chronic lung inflammation and persistent pathology. Am J Respir Cell Mol Biol 26, 152-159.

Vincent, A.M., Perrone, L., Sullivan, K.A., Backus, C., Sastry, A.M., Lastoskie, C., Feldman, E.L., 2007. Receptor for advanced glycation end products activation injures primary sensory neurons via oxidative stress. Endocrinology 148, 548-558.

Wautier, J.L., Schmidt, A.M., 2004. Protein glycation: a firm link to endothelial cell dysfunction. Circ Res 95, 233-238.

Widdicombe, J.H., Wine, J.J., 2015. Airway Gland Structure and Function. Physiol Rev 95, 1241-1319.

Wine, J.J., 2007. Parasympathetic control of airway submucosal glands: central reflexes and the airway intrinsic nervous system. Auton Neurosci 133, 35-54.

Yamamoto, Y., Harashima, A., Saito, H., Tsuneyama, K., Munesue, S., Motoyoshi, S., Han, D., Watanabe, T., Asano, M., Takasawa, S., Okamoto, H., Shimura, S., Karasawa, T., Yonekura, H., Yamamoto, H., 2011. Septic shock is associated with receptor for advanced glycation end products ligation of LPS. J Immunol 186, 3248-3257.

Yan, S.F., Ramasamy, R., Schmidt, A.M., 2010. The RAGE axis: a fundamental mechanism signaling danger to the vulnerable vasculature. Circ Res 106, 842-853.

Yanagihara, K., Seki, M., Cheng, P.W., 2001. Lipopolysaccharide Induces Mucus Cell Metaplasia in Mouse Lung. Am J Respir Cell Mol Biol 24, 66-73.

Yu, X., Shen, N., Zhang, M.L., Pan, F.Y., Wang, C., Jia, W.P., Liu, C., Gao, Q., Gao, X., Xue, B., Li, C.J., 2011. Egr-1 decreases adipocyte insulin sensitivity by tilting PI3K/Akt and MAPK signal balance in mice. EMBO J 30, 3754-3765.

Zhang, L., Katselis, G.S., Moore, R.E., Lekpor, K., Goto, R.M., Lee, T.D., Miller, M.M., 2011. Proteomic analysis of surface and endosomal membrane proteins from the avian LMH epithelial cell line. J Proteome Res 10, 3973-3982.

Zhang, X., Douglas, K.L., Jin, H., Eldaif, B.M., Nassar, R., Fraser, M.O., Dolber, P.C., 2008. Sprouting of substance P-expressing primary afferent central terminals and spinal micturition reflex NK1 receptor dependence after spinal cord injury. Am J Physiol Regul Integr Comp Physiol 295, R2084-2096.

Zhou, Y., Jiang, Y.Q., Wang, W.X., Zhou, Z.X., Wang, Y.G., Yang, L., Ji, Y.L., 2012. HMGB1 and RAGE levels in induced sputum correlate with asthma severity and neutrophil percentage. Hum Immunol 73, 1171-1174.